DISCLAIMER

Developers and distributors assume no responsibility for the use of MIDAS Family Program (midas Civil, midas FEA, midas FX+, midas Gen, midas Drawing, midas SDS, midas GTS, SoilWorks, midas NFX ; hereinafter referred to as “MIDAS package”) or for the accuracy or validity of any results obtained from the MIDAS package.

.5

Developers and distributors shall not be liable for loss of profit, loss of business, or financial loss which may be caused directly or indirectly by the MIDAS package, when used for any purpose or use, due to any defect or deficiency therein. Accordingly, the user is encouraged to fully understand the bases of the program and become familiar with the users manuals. The user shall also independently verify the results produced by the program.

Part I

Constitutive Models

Chapter 1 Introduction to Constitutive Models

Chapter 2 Structural Constitutive Models

Chapter 3 Ground Constitutive Models

Chapter 4 Seepage Constitutive Models

Constitutive Models

Chapter 1 **Introduction to Constitutive Models / 001**

1.1 General / 001
1.2 Yield Criteria for Elasto-plastic Models / 003
1.2.1 Stress Invariants / 003

Chapter 2 **Structural Constitutive Models / 008**

2.1 Geotextile Model for Linear Elements / 008
2.2 Nonlinear Elastic Behavior of Elastic Link Element / 009
2.3 Interface Model / 010
2.3.1 Introduction / 010
2.3.2 Material Properties / 010
2.3.3 Details of Interface Model / 011
2.4 Pile Nonlinear Model / 014
2.4.1 Introduction / 014
2.4.2 Material Properties / 015
2.4.3 Nonlinear Elastic Behavior / 015
2.5 Interface Behaviors for Anchor, Rockbolt and Nail / 018
2.5.1 Introduction / 018
2.5.2 Material Properties / 020
2.5.3 Material Behaviors / 021

Chapter 3 **Ground Constitutive Models / 025**

3.1 Linear Elastic Model / 025
3.1.1 Introduction / 025

3.1.2 Material Properties / 026
3.2 Tresca Model / 028
3.2.1 Introduction / 028
3.2.2 Material Properties / 028
3.2.3 Yield Function / 029
3.3 von Mises Model / 032
3.3.1 Introduction / 032
3.3.2 Material Properties / 032
3.3.3 Yield Function / 032
3.4 Mohr-Coulomb Model / 035
3.4.1 Introduction / 035
3.4.2 Material Properties / 036
3.4.3 Yield Function / 037
3.5 Drucker-Prager Model / 041
3.5.1 Introduction / 041
3.5.2 Material Properties / 041
3.5.3 Yield Function / 041
3.6 Hyperbolic Model (Duncan-Chang Model) / 045
3.6.1 Introduction / 045
3.6.2 Material Properties / 046
3.6.3 Initial Modulus / 047
3.6.4 Tangential Modulus / 048
3.6.5 Unloading-Reloading Modulus / 049
3.6.6 Poisson's Ratio / 049
3.6.7 Yielding Zone / 050
3.7 Hoek-Brown Model / 052
3.7.1 Introduction / 052
3.7.2 Material Properties / 052
3.7.3 Yield Function / 052
3.8 Modified Cam-Clay Model / 055
3.8.1 Introduction / 055

3.8.2 Material Properties / 056
3.8.3 Yield Function / 059
3.8.4 Initial Condition / 061
3.9 Sekiguchi-Ohta Model / 064
3.9.1 Introduction / 064
3.9.2 Material Properties / 064
3.9.3 Yield Function / 071
3.9.4 Initial Condition / 073
3.10 Modified Mohr-Coulomb Model / 075
3.10.1 Introduction / 075
3.10.2 Material Properties / 075
3.10.3 Non-Linear Elasticity / 076
3.10.4 Failure criterion / 077
3.10.5 Flow Rule / 078

Chapter 4 **Seepage Constitutive Models / 080**
4.1 Permeability Coefficient Function / 080
4.2 Volumetric Water Content Function / 081
4.3 Consecutive Function / 083

Appendix / 084
A. Output of Safety Ratio / 084
B. Output of Plastic State / 086

Chapter 1

Introduction to Constitutive Models

1.1 General

The constitutive models available in SoilWorks are classified based on the purposes of their usage as follows:

1) Structural constitutive models

- ✓ Nonlinear elastic model for elastic link
- ✓ Geotextile model
- ✓ Interface Behavior model
- ✓ Pile nonlinear model
- ✓ Interface Behavior Model for Rockbolt, Anchor and Nail

2) Geotechnical constitutive models

- ✓ Linear elastic model
- ✓ Tresca model
- ✓ von Mises model
- ✓ Mohr-Coulomb model
- ✓ Drucker-Prager model
- ✓ Hyperbolic model (Duncan-Chang model)
- ✓ Hoek-Brown model
- ✓ Modified Cam-Clay model
- ✓ Sekiguchi-Ohta model

3) Seepage constitutive models

- ✓ Permeability coefficient function
- ✓ Volumetric water content function
- ✓ Consecutive function

The structural and geotechnical constitutive models above can be grouped into (linear and nonlinear) elastic and elasto-plastic models depending on the characteristics of material behaviors.

A. Elastic constitutive model

A-1. Linear elastic constitutive model

- ✓ Linear elastic model

A-2. Nonlinear elastic constitutive model

- ✓ Nonlinear elastic model for elastic link
- ✓ Geotextile model of linear elements
- ✓ Pile nonlinear model

B. Elasto-plastic constitutive model

- ✓ Interface model
- ✓ Interface behavior model for anchor, rockbolt and nail
- ✓ Tresca
- ✓ von Mises
- ✓ Mohr-Coulomb
- ✓ Drucker-Prager
- ✓ Hyperbolic model (Duncan-Chang model)
- ✓ Hoek-Brown model
- ✓ Modified Cam-Clay model
- ✓ Sekiguchi-Ohta model

C. Visco Elasto-plastic constitutive model

- ✓ Sekiguchi-Ohta model

Analysis algorithms of nonlinear elastic and elasto-plastic constitutive models can be found in Section 1.3 Nonlinear Analysis of Tunnel Manual. In the rest of this chapter, yield criteria for elasto-plastic constitutive models are described. Structural constitutive models are subsequently described in Chapter 2. Finally, geotechnical and seepage constitutive models are described in Chapter 3 and Chapter 4 respectively.

1.2 Yield Criteria for Elasto-plastic Models

Difficulties arise in geometrically or physically expressing a yield function by the commonly used multi-axial stress components. Accordingly, the yield function is generally defined in terms of the components, which are independent of the stress coordinate system. The yield condition is defined using the principal stresses as follows:

$$f\left(\sigma_1, \sigma_2, \sigma_3\right) = 0 \tag{1.2.1}$$

One of the convenient methods to express a yield function is to use stress invariants.

1.2.1 Stress Invariants

1.2.1.1 Stress Invariants

The stress state at a given point within a material can be expressed using the stress tensor, σ_{ij}. The following equation is given using the direction vector, n_j, which defines the principal stress direction.

$$\left(\sigma_{ij} - \sigma\delta_{ij}\right) n_j = 0 \tag{1.2.2}$$

where, δ_{ij} : Kronecker delta

In order to obtain a non-zero solution for n_j in Eq. (1.2.1) while satisfying Eq. (1.2.2), the following condition needs to be met.

$$\left|\sigma_{ij} - \sigma\delta_{ij}\right| = 0 \tag{1.2.3}$$

The matrix Eq. (1.2.3) can be expressed in a cubic equation of principal stresses.

$$\sigma^3 - I_1\sigma^2 + I_2\sigma - I_3 = 0 \tag{1.2.4}$$

where,

$$
\begin{aligned}
I_1 &= \sigma_x + \sigma_y + \sigma_z = \sigma_{ii} \\
I_2 &= \left(\sigma_x\sigma_y + \sigma_y\sigma_z + \sigma_z\sigma_x\right) - \left(\tau_{xy}^2 + \tau_{yz}^2 + \tau_{zx}^2\right) = \frac{1}{2}\left(I_1^2 - \sigma_{ij}\sigma_{ji}\right) \\
I_3 &= \begin{vmatrix} \sigma_x & \tau_{xy} & \tau_{xz} \\ \tau_{yx} & \sigma_y & \tau_{yz} \\ \tau_{zx} & \tau_{zy} & \sigma_z \end{vmatrix} = \frac{1}{3}\sigma_{ij}\sigma_{jk}\sigma_{ki} - \frac{1}{2}I_1\sigma_{ij}\sigma_{ji} + \frac{1}{6}I_1^3
\end{aligned}
\tag{1.2.5}
$$

The principal stresses, σ_1, σ_2 and σ_3, can be combined to form the first, second, and third stress invariants, I_1, I_2 and I_3 respectively.

$$
\begin{aligned}
I_1 &= \sigma_1 + \sigma_2 + \sigma_3 \\
I_2 &= \sigma_1\sigma_2 + \sigma_2\sigma_3 + \sigma_3\sigma_1 \\
I_3 &= \sigma_1\sigma_2\sigma_3
\end{aligned}
\tag{1.2.6}
$$

1.2.1.2 Deviatoric Stress Invariants

The stress tensor, σ_{ij} can be expressed using two other stress tensors, hydrostatic stress tensor (σ_m) and deviatoric stress tensor (s_{ij}).

$$\sigma_{ij} = s_{ij} + \sigma_m\delta_{ij} \tag{1.2.7}$$

The hydrostatic stress tensor represents the state of volume change meaning the average stress, while the deviatoric stress tensor represents the state of distortion in a pure shear state.

In order to calculate the deviatoric stress invariants, the following equation needs to be solved as was done to calculate the stress invariants from Eq. (1.2.3).

$$\left|s_{ij} - s\delta_{ij}\right| = 0 \tag{1.2.8}$$

Expressing Eq. (1.2.8) in the form of an equation, it can be written as,

$$s^3 - J_1 s^2 + J_2 s - J_3 = 0 \tag{1.2.9}$$

where,

$$
\begin{aligned}
J_1 &= s_{ii} = s_x + s_y + s_z = 0 \\
J_2 &= \frac{1}{2} s_{ij} s_{ji} \\
&= \frac{1}{6}\left[\left(\sigma_x - \sigma_y\right)^2 + \left(\sigma_y - \sigma_z\right)^2 + \left(\sigma_z - \sigma_x\right)^2\right] + \tau_{xy}^2 + \tau_{yz}^2 + \tau_{zx}^2 \\
J_3 &= \frac{1}{3} s_{ij} s_{jk} s_{ki} = \begin{vmatrix} s_x & \tau_{xy} & \tau_{xz} \\ \tau_{yx} & s_y & \tau_{yz} \\ \tau_{zx} & \tau_{zy} & s_z \end{vmatrix}
\end{aligned}
\tag{1.2.10}
$$

The deviatoric principal stresses, s_1, s_2 and s_3, can be combined to form the first, second, and third deviatoric stress invariants, J_1, J_2 and J_3 respectively.

$$
\begin{aligned}
J_1 &= s_1 + s_2 + s_3 = 0 \\
J_2 &= \frac{1}{2}\left(s_1^2 + s_2^2 + s_3^2\right) = \frac{1}{6}\left[\left(\sigma_1 - \sigma_2\right)^2 + \left(\sigma_2 - \sigma_3\right)^2 + \left(\sigma_3 - \sigma_1\right)^2\right] \\
J_3 &= \frac{1}{3}\left(s_1^3 + s_2^3 + s_3^3\right) = s_1 s_2 s_3
\end{aligned}
\tag{1.2.11}
$$

I_1, I_2, I_3, J_1, J_2 and J_3, are invariants of scalar values independent of the orientation of the coordinate system. The three invariants, I_1, J_2, and J_3, are primarily used to define the yield function (yield surface) because of its simplicity in geometry.

1.2.1.3 Geometric Meaning of the Three Stress Invariants

Yielding in most material models is mainly governed by the deviatoric stresses. Accordingly, decomposing the yield function into hydrostatic and deviatoric stress components serves to very conveniently define the geometric shape of the yield function.

The following describes the method of decomposing the stress state at a point, $\mathbf{P}\left(\sigma_1,\ \sigma_2,\ \sigma_3\right)$ into a hydrostatic pressure axis and a deviatoric stress axis.

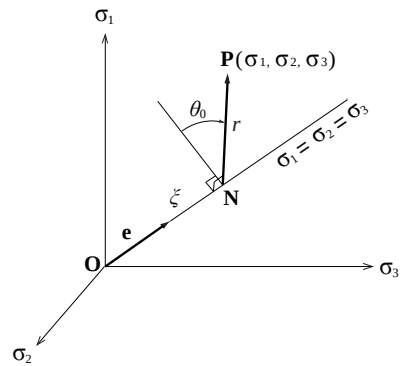

Figure 1.2.1 State of stress in the principal stress space

As shown in Figure 1.2.1, the stress state represented as the point P can be defined as a vector, **OP** in the principal stress coordinate system. This vector, **OP** can be decomposed into two vectors, **ON** along the hydrostatic pressure axis and **NP** on the deviatoric plane perpendicular to the hydrostatic pressure axis. The magnitude of each vector is given by,

$$\begin{aligned} |\mathbf{ON}| &= \xi = \frac{1}{\sqrt{3}} I_1 \\ |\mathbf{NP}| &= r = \sqrt{2J_2} \end{aligned} \tag{1.2.12}$$

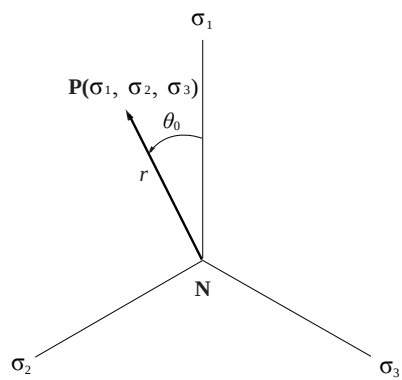

Figure 1.2.2 State of stress on the deviatoric plane (Projection of the stress on the deviatoric plane)

Figure 1.2.2 shows the deviatoric plane perpendicular to the hydrostatic pressure axis. In order to define the state of stress at the point P on the deviatoric plane, the vector NP must be rotated by θ_0 from the σ_1 axis. Angle θ_0 is referred to as the similarity angle and can be expressed as,

$$\theta_0 = \frac{1}{3}\cos^{-1}\left(\frac{3\sqrt{3}}{2}\frac{J_3}{J_2^{3/2}}\right) \tag{1.2.13}$$

The angle, θ_0 has the following range:

$$0 \le \theta_0 \le \frac{\pi}{3} \tag{1.2.14}$$

For numerical analysis, using the Lode's angle (θ) is more convenient than using the similarity angle, θ_0.

$$\theta = \frac{1}{3}\sin^{-1}\left(-\frac{3\sqrt{3}}{2}\frac{J_3}{J_2^{3/2}}\right) \tag{1.2.15}$$

where, $\theta = \theta_0 - \frac{\pi}{6}$ for the following range:

$$-\frac{\pi}{6} \le \theta \le \frac{\pi}{6} \tag{1.2.16}$$

In defining the yield function of a material, it is often useful to express the principal stresses using the stress invariants. The principal stresses are rearranged using the Lode's angle as,

$$\begin{Bmatrix}\sigma_1\\ \sigma_2\\ \sigma_3\end{Bmatrix} = \frac{2\sqrt{J_2}}{\sqrt{3}}\begin{Bmatrix}\sin\left(\theta + \frac{2}{3}\pi\right)\\ \sin(\theta)\\ \sin\left(\theta + \frac{4}{3}\pi\right)\end{Bmatrix} + \frac{I_1}{3}\begin{Bmatrix}1\\1\\1\end{Bmatrix} \tag{1.2.17}$$

Chapter 2

Structural Constitutive Models

2.1 Geotextile Model for Linear Elements

SoilWorks provides a geotextile model, which is a linear element used for ground reinforcement and is a truss element limited to tension-only behavior. The tension-only behavior is generally defined as a nonlinear elastic model or an elasto-plastic model. SoilWorks defines the geotextile behavior as a nonlinear elastic model for the sake of convenience.

The nonlinear elastic behavior model provided by SoilWorks can be defined using a multi-linear function. The tension-only behavior is depicted in Figure 2.1.1.

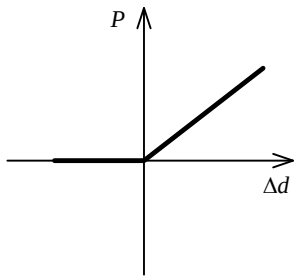

Figure 2.1.1 Tension-only behavior

In Figure 2.1.1, Δd represents the relative displacement between the connected nodes, and P represents the internal member force.

2.2 Nonlinear Elastic Behavior of Elastic Link Element

SoilWorks supports the following behavior models to represent elastic link elements:

- ✓ General
- ✓ Rigid
- ✓ Tension-only
- ✓ Compression-only

The general behavior defines the interactive movements of two connected nodes using the defined stiffness between the nodes. The rigid behavior simulates rigid body motion between two nodes by assigning a very large stiffness value between the nodes. This rigid behavior is essentially the same as that of a rigid link element, except that the relationship of a master node and a slave node does not exist unlike a rigid link element.

The compression-only or tension-only behavior is similar to that of the nonlinear elastic behavior of the geotextile model for linear elements as discussed in Chapter 2.1. The nonlinear behavior is defined using the force-displacement relationship as shown in Figure 2.2.1.

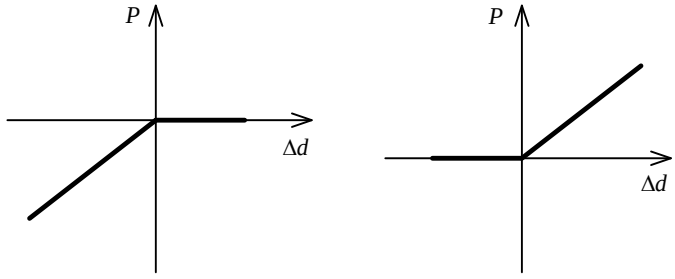

(a) Compression-only model (b) Tension-only model

Figure 2.2.1 Nonlinear elastic behaviors of elastic link elements

In Figure 2.2.1, Δd represents the relative displacement between the connected nodes, and P represents the internal member force.

2.3 Interface Model

2.3.1 Introduction

SoilWorks provides an interface model, which is used to simulate the behavior between homogeneous materials or heterogeneous materiasl. Although it is classified as a structural constitutive model, it can be used to model ground behaviors including rock joints or bedding of strata. The interface model is used to simulate various types of interface behaviors not only in geotechnical engineering but also in the architectural and civil engineering fields. The interface model is based on the Coulomb's law (1785) in which the friction at the interface is proportional to the coefficient of friction and the magnitude of the normal force acting on the interface.

The main applications include the interface between (1) pile and surrounding soils, (2) retaining wall and supported soils, (3) lining and ground, and (4) jointed rocks or fault zones. This model can be also used to simulate brick and mortar in masonry buildings, discrete cracking in concrete, and bond-slip between steel and concrete.

2.3.2 Material Properties

The material properties required to define the interface behavior between homogeneous or heterogeneous materials based on the Coulomb friction are listed in Table 2.3.1.

Table 2.3.1 Material property parameters for Coulomb friction

Input parameters
Normal stiffness modulus (k_n)
Shear stiffness modulus (k_t)
Cohesion (c)
Internal friction angle (ϕ)
Tensile strength for tension cut-off
Reduced shear stiffness for Mode-II model
Cohesion multilinear hardening function
Friction angle multilinear hardening function

2.3.3 Details of Interface Model (Coulomb Friction Model)

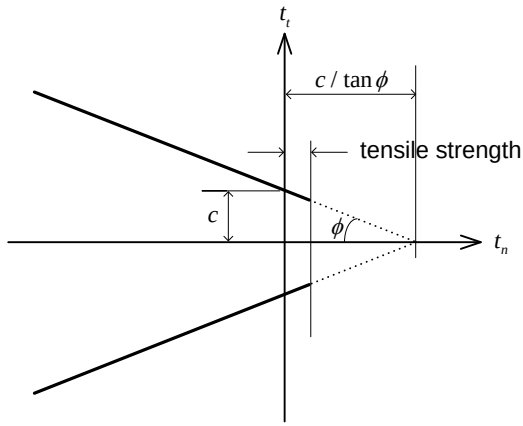

Figure 2.3.1 Yield surface for Coulomb friction

The failure function (f) and the potential function (g) in the Coulomb friction model are defined using three coefficients, ϕ , c and ψ as presented in Eq. (2.3.1). These coefficients represent the friction angle, cohesion and dilatancy angle respectively. Figure 2.3.1 exhibits the yield surface for the Coulomb friction model in a 2D plane.

$$\begin{cases} f = \sqrt{t_t^2} + t_n \tan\phi(\kappa) - c(\kappa) = 0 \\ g = \sqrt{t_t^2} + t_n \tan\psi \end{cases} \tag{2.3.1}$$

where,

$\phi(k)$	:	Internal friction angle defined as a function of deformation history parameter, κ
$c(k)$	:	Cohesion defined as a function of deformation history parameter, κ
ψ	:	Dilatancy angle (a constant under a given normal stress)

The plastic relative displacement ($\Delta\dot{\mathbf{u}}^p$) is defined with the plastic multiplier ($\dot{\lambda}$) and the component of the plastic direction.

$$\Delta\dot{\mathbf{u}}^p = \dot{\lambda}\frac{\partial g}{\partial \mathbf{t}} \tag{2.3.2}$$

The first-order Taylor series expansion for the yield function (f) is used to define the plastic response behavior of a structure resisting external force, which can be expressed in the form of a rate of increase as below.

$$\dot{f} = \left(\frac{\partial f}{\partial \mathbf{t}}\right)^T \dot{\mathbf{t}} + \frac{\partial f}{\partial \kappa}\dot{\kappa} = 0 \tag{2.3.3}$$

Substituting Eq. (2.3.1) and Eq. (2.3.2) into Eq. (2.3.3), the plastic multiplier ($\dot{\lambda}$) can be obtained as follows:

$$\dot{\lambda} = \frac{\left(\frac{\partial f}{\partial \mathbf{t}}\right)^T \mathbf{D}^e}{-\frac{\partial f}{\partial \kappa} + \left(\frac{\partial f}{\partial \mathbf{t}}\right)^T \mathbf{D}^e \frac{\partial g}{\partial \mathbf{t}}}\Delta\dot{\mathbf{u}} = \frac{\left(\frac{\partial f}{\partial \mathbf{t}}\right)^T \mathbf{D}^e}{-h + \left(\frac{\partial f}{\partial \mathbf{t}}\right)^T \mathbf{D}^e \frac{\partial g}{\partial \mathbf{t}}}\Delta\dot{\mathbf{u}} \tag{2.3.4}$$

where, h is the hardening parameter.

The incremental internal parameter ($\dot{\kappa}$) is defined as the absolute value of the plastic relative displacement, and is related to the increase in the plastic multiplier ($\dot{\lambda}$) as,

$$\dot{\kappa} = \left|\Delta\dot{\mathbf{u}}_t^p\right| = \dot{\lambda}\left|\frac{\partial g}{\partial \mathbf{t}}\right| = \dot{\lambda}\sqrt{\left(\frac{\partial g}{\partial \mathbf{t}}\right)^T \cdot \left(\frac{\partial g}{\partial \mathbf{t}}\right)} = \dot{\lambda}\sqrt{1+\tan^2\psi} = \dot{\lambda} \quad \because \tan\psi << 1 \tag{2.3.5}$$

where,

$$\partial g / \partial \mathbf{t} = \left\{\tan\psi \quad t_t / |t_t|\right\} \tag{2.3.6}$$

By substituting Eq. (2.3.4) and Eq. (2.3.6) into Eq. (2.3.3), the traction rate vector (increase in stress) can be expressed as Eq. (2.3.7).

$$\dot{\mathbf{t}} = \left\{ \mathbf{D}^e - \frac{\mathbf{D}^e \dfrac{\partial g}{\partial \mathbf{t}} \left(\dfrac{\partial f}{\partial \mathbf{t}} \right)^T \mathbf{D}^e}{-h + \left(\dfrac{\partial f}{\partial \mathbf{t}} \right)^T \mathbf{D}^e \dfrac{\partial g}{\partial \mathbf{t}}} \right\} \Delta \dot{\mathbf{u}} \tag{2.3.7}$$

where,

$$\mathbf{D}^e = \begin{bmatrix} k_n & 0 \\ 0 & k_t \end{bmatrix}$$

$$h = \frac{\partial f}{\partial \kappa} = \frac{\partial f}{\partial \mathbf{t}} \frac{\partial \mathbf{t}}{\partial \Delta \mathbf{u}_t^p} \frac{\partial \Delta \mathbf{u}_t^p}{\partial \kappa}$$

$$\frac{\partial g}{\partial \mathbf{t}} = \left\{ \tan\psi \quad \frac{t_t}{|t_t|} \right\}$$

$$\left(\frac{\partial f}{\partial \mathbf{t}} \right)^T = \left\{ \tan\phi(k) \quad \frac{t_t}{|t_t|} \right\}$$

Rearranging Eq. (2.3.8), it can be written as,

$$\dot{\mathbf{t}} = \frac{1}{-h + k_n \tan\phi \tan\psi + k_t} \begin{bmatrix} k_n(h + k_t) & -k_n k_t \tan\psi \dfrac{t_t}{|t_t|} \\ -k_n k_t \tan\phi(k) \dfrac{t_t}{|t_t|} & k_t(h + k_n \tan\phi \tan\psi) \end{bmatrix} \Delta \dot{\mathbf{u}} \tag{2.3.8}$$

If the internal friction is equal to the dilatancy angle ($\phi = \psi$), the tangent stiffness matrix in the bracket becomes symmetric generating an associated plastic flow in the model. This case does not coincide with the true behavior because the excessive fracture opening behavior can be induced in the direction normal to the interface.

If the internal friction angle is not equal to the dilatancy angle ($\phi \neq \psi$), the tangent stiffness matrix in the bracket becomes non-symmetric generating a non-associated plastic flow in the model. In this case, the analysis may take considerable time due to the increased size of memory of the stiffness matrix resulting in slow execution. It should be noted that if the difference between the internal friction angle and the dilatancy angle is large (that is, non-associativity is large), the analysis will likely diverge. Therefore, SoilWorks recommends that the difference between the two angles be no more than 20 degrees ($\phi - \psi \leq 20°$).

2.4 Pile Nonlinear Model

2.4.1 Introduction

The behavior of the pile element is described by the interface behavior between the mother elements of the ground and beam/truss elements of a pile. The interface behavior of a pile exhibits in the two normal directions and the tangential direction to the pile. The behavior in the two normal directions is assumed to act as a fully integrated rigid body between the pile and the mother elements. In the tangential direction, a nonlinear elastic behavior is assumed.

The behavior at the pile tip is also considered as the interface behavior between mother elements and a node at the pile tip. The rigid body behavior between the mother elements and the pile tip is assumed in the normal directions to the pile, and the nonlinear elastic behavior is assumed in the tangential direction. The shape of each element associated with the local coordinate system is described in the Tunnel manual.

In SoilWorks, the interface behavior of a pile is defined using the nonlinear elastic behavior as described in Chapter 2.4.3.

2.4.2 Material Properties

The required parameters for pile element modeling are listed in Table 2.4.1.

Table 2.4.1 Input material property parameters for pile and pile tip models

Input parameters	Remarks
Ultimate shear force	
Shear Stiffness Modulus	Stiffness in shear direction
Function	Pile shear function
Normal Stiffness Modulus (Kn)	Stiffness in normal direction
Reference Height	Reference height of pile element
Slope of Friction-Rel. Disp. Curve	Rate of change in relationship curve between relative displacement and friction based on locations
Tip Bearing Capacity	Pile tip capacity
Tip Spring Stiffness	Pile tip stiffness
Function	Function of pile tip element

2.4.3 Nonlinear Elastic Behavior

The behavior in the tangential direction is of the main interest in SoilWorks, which is defined as a nonlinear elastic behavior. The behavior in the normal directions is defined as a linear elastic behavior.

The nonlinear elastic behavior at the interface of the pile element and the pile tip element in the tangential direction can be defined by the ultimate shear force or in the form of a function.

In the case of defining the nonlinear elastic behavior by the ultimate shear force, Figure 2.4.1 of an elasto perfectly-plastic behavior is assumed in which the shear stiffness and ultimate force varies with depth.

If the nonlinear elastic behavior is defined in the form of a function, the constitutive equation is formulated by a user-defined slope of the relative displacement - friction curve.

Figure 2.4.2 represents the variation of the shear stiffness relative to the depth. In order to estimate the interface strength at a given depth, the user needs to adjust the relative displacement-friction curve at the reference depth (Fig 2.4.1). The modified relationships can be formulated as Eq. (2.4.1).

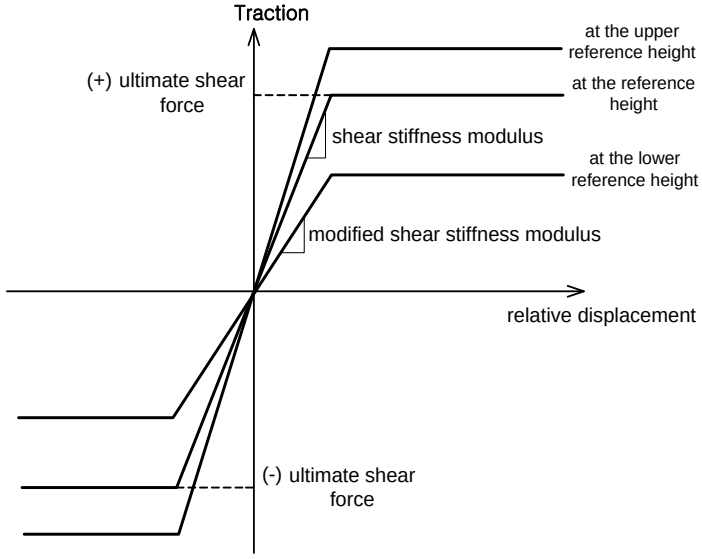

Figure 2.4.1 Relationship between relative displacement and traction

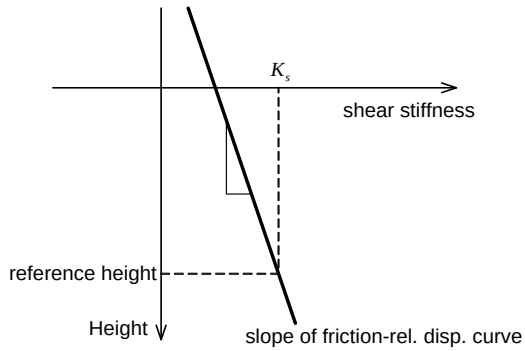

Figure 2.4.2 Variation of shear stiffness at reference height

$$k_s = k_s^{ref} + (y^{ref} - y) \times k_s^{inc}$$
$$f = 1 + a \cdot \frac{\left(y - y_{ref}\right)}{t} \qquad (2.4.1)$$

where,

k_s	: Shear stiffness in tangential direction
y^{ref}	: Reference depth
k_s^{ref}	: Shear stiffness at reference depth
k_s^{inc}	: Increment of shear stiffness
y	: Integration point at a given depth
f	: Factor of increase in stiffness
a	: Slope of relative displacement-friction curve
t	: Ultimate shear force

The factor of increase in stiffness applies not only to the stiffness, but also applies to the ultimate shear force. Note that the direction of depth is in the negative Z direction as shown in Figure 2.4.2.

2.5 Interface Behaviors for Anchor, Rockbolt and Nail

2.5.1 Introduction

Anchor, rockbolt and nail elements are 1-dimensional elements embedded in ground with the inclusion of interface elements between 1-dimensional elements and ground elements. Truss elements represent the 1-dimensional elements, and line interface elements are used over the bond length between the truss elements and the ground elements. The anchor element consists of free length and bond length as shown in Figure 2.5.1. Unlike the anchor element, the entire interface of rockbolt and nail elements fully corresponds to bond length.

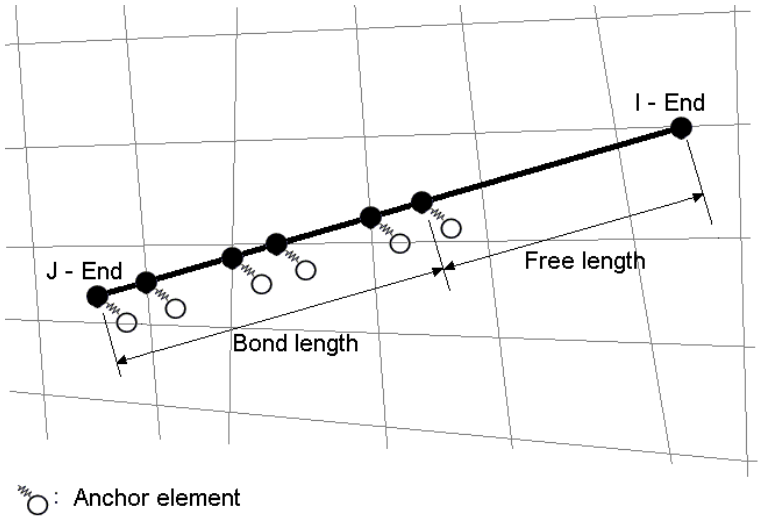

Figure 2.5.1 Anchor element

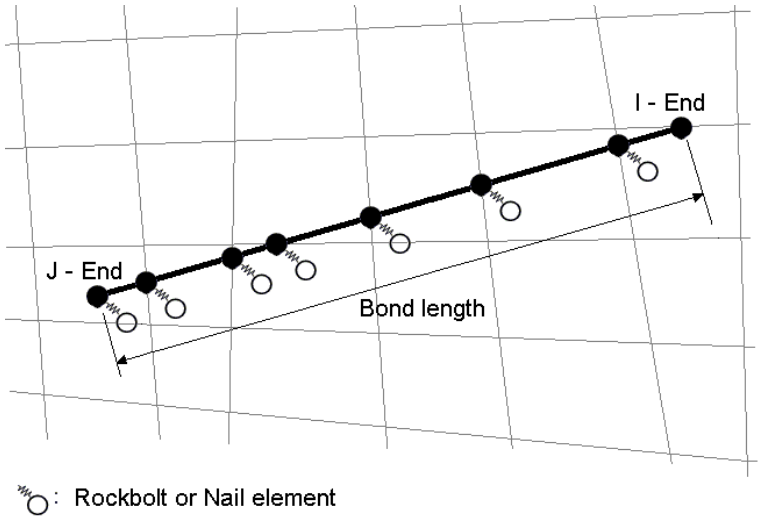

Figure 2.5.2 Rockbolt or nail element

2.5.2 Material Properties

The required material property parameters to define anchor, rockbolt and nail elements are listed in Table 2.5.1.

Table 2.5.1 Material properties required for anchor elements

Material	Property	Unit
Reinforcement	Elastic modulus	N / mm^2
	Compressive yield strength	MPa
	Tensile yield strength	MPa
	Diameter	mm
	Internal node number at bond length	
	Bond length	mm
Grout	Grout compressive strength	MPa
	Grout shear modulus	MPa
	Grout friction angle	$Degree$
	Grout annulus thickness	mm
Ground	Compressive strength	MPa

Table 2.5.2 Material properties required for rockbolt and nail elements

Material	Property	Unit
Reinforcement	Elastic modulus	N / mm^2
	Compressive yield strength	MPa
	Tensile yield strength	MPa
	Diameter	mm
Grout	Grout compressive strength	MPa
	Grout shear modulus	MPa
	Grout friction angle	$Degree$
	Grout annulus thickness	mm
Ground	Compressive strength	MPa

2.5.3 Material Behaviors

The behaviors of 1-dimensional elements such as anchor, rockbolt and nail elements are described in Constitutive Model of the midas GTS manual. In this chapter, only the material behavior of the interface element is discussed. The material behavior of the interface element is governed by the shear behavior between the reinforcement and the ground. The interface behavior can be defined by the elasto-perfectly-plastic model using the relative displacement between the reinforcement and grout or the grout and rock as shown in Figure 2.5.3.

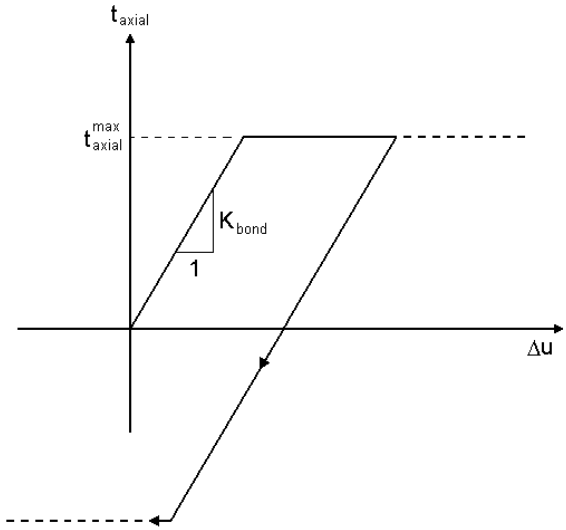

(a) Unloading

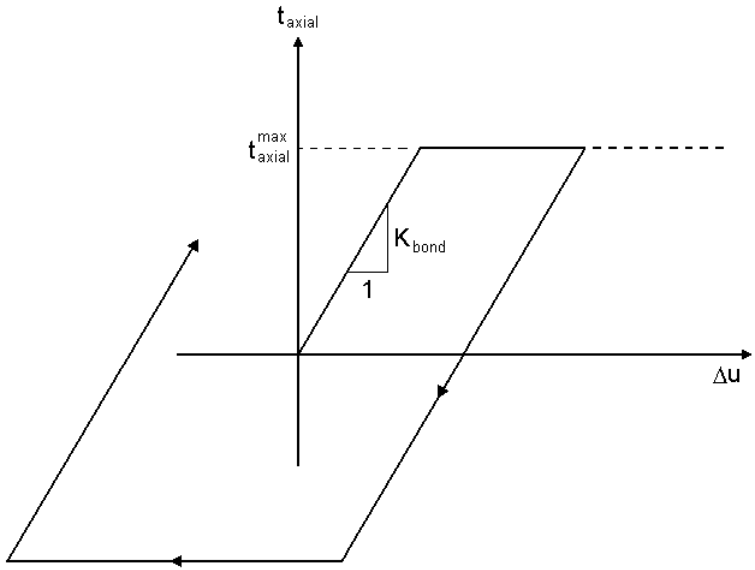

(b) Reloading

Figure 2.5.3 Shear behavior of grout

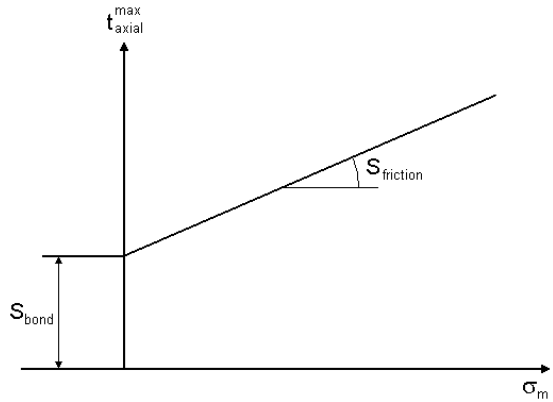

Figure 2.5.4 Maximum shear strength of grout

K_{bond} can be directly obtained from field pull-out tests. However, if desirable test results are not available, an approximate value of K_{bond} from the following equation can be used:

$$K_{bond} = \frac{2\pi G}{10\ln\left(1+2t_G / D\right)\pi D} \tag{2.5.1}$$

where, G is the shear modulus of grout, t_G is the thickness of grout, and D is the diameter of the reinforcement.

The maximum shear strength of the grout and the friction angle can be also determined from tests. As shown in Figure 2.5.4, the maximum shear strength is assumed to linearly increase with the magnitude of effective confining pressure, σ'_m , which is expressed as,

$$t_{axial}^{\max} = S_{bond} + S_{friction} \times \sigma'_m \tag{2.5.2}$$

where, $S_{friction}$ is the friction angle of the grout, and σ'_m is the effective confinement pressure.

S_{bond} is determined by the lesser of the shear strength of the ground and the shear strength of the grout. Approximately 1/2 of the uniaxial compressive strength can be used

for the shear strengths of the ground and grout.

The effective confinement pressure, σ'_m represents the confining stress acting on the plane normal to the axis of the reinforcement at the reinforcement node, which is obtained by interpolating the stresses of soil elements connected to the node. σ'_m is given by,

$$\sigma'_m = -\left(\frac{\sigma_{nn} + \sigma'_{zz}}{2} + p \right) \tag{2.5.3}$$

where,

$$\sigma_{nn} = \sigma'_{xx} n_1^2 + \sigma'_{yy} n_2^2 + 2\sigma_{xy} n_1 n_2$$

σ'_{zz} is out-of-plane stress, p is pore water pressure, and n_i is directional cosine in the direction of the reinforcement axis.

Chapter 3

Ground Constitutive Models

3.1 Linear Elastic Model

3.1.1 Introduction

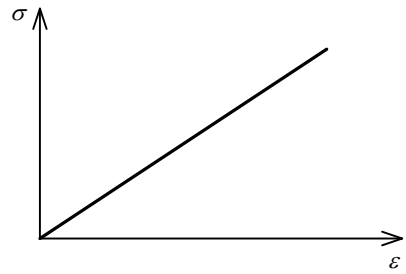

Figure 3.1.1 Linear elastic stress-strain behavior

The simplest constitutive model in SoilWorks is the linear elastic model in which stress is directly proportional to stain as shown in Figure 3.1.1. The proportional coefficients are the modulus of elasticity (E) and Poisson's ratio (ν). In 3D analysis, the stress-strain relationship can be expressed using the following equation:

$$\begin{Bmatrix} \sigma_x \\ \sigma_y \\ \sigma_z \\ \tau_{xy} \\ \tau_{yz} \\ \tau_{zx} \end{Bmatrix} = \frac{E}{(1+\nu)(1-2\nu)} \begin{bmatrix} 1-\nu & \nu & \nu & & & \\ \nu & 1-\nu & \nu & & & \\ \nu & \nu & 1-\nu & & & \\ & & & \frac{1-2\nu}{2} & & \\ & & & & \frac{1-2\nu}{2} & \\ & & & & & \frac{1-2\nu}{2} \end{bmatrix} \begin{Bmatrix} \varepsilon_x \\ \varepsilon_y \\ \varepsilon_z \\ \gamma_{xy} \\ \gamma_{yz} \\ \gamma_{zx} \end{Bmatrix} \tag{3.1.1}$$

In 2D analysis, $\tau_{yz} = \tau_{zx} = \gamma_{yz} = \gamma_{zx} = 0$, and especially for plane strain analysis, $\varepsilon_z = 0$. As ν approaches 0.5, the terms $(1-2\nu)/2$ and $(1-\nu)$ approach 0 (zero) and ν

respectively. This indicates that the stress-strain relationship depends on the constant (ν) that represents the pure volumetric strain. In addition, as $(1-2\nu)$ approaches zero, $E/\left[(1+\nu)(1-2\nu)\right]$ turns into infinity. From the physical viewpoint, it means that the volumetric strain becomes close to zero as ν approaches 0.5.

For numerical analysis, the Poisson's ratio (ν) must not be equal to 0.5. A Poisson's ratio greater than 0.49 may cause numerical instability. Even though SoilWorks does not permit the Poisson's ratio equal to or greater than 0.5, there is no additional limitation to prevent numerical instability. In case of incompressible solid elements, the user may specify the Poisson's ratio close to 0.5 and make judgment on whether or not any numerical error has occurred from the analysis results. In case of undrained conditions, the "undrained" option should be used as explained in Part 4, instead of setting the Poisson ration close to 0.5.

3.1.2 Material Properties

The input data for the linear elastic model is listed in Table 3.1.1.

Table 3.1.1 Input data for linear elastic model

Input Parameters	Remarks
Modulus of Elasticity (E)	
Poisson's Ratio (ν)	
Inc. of Elastic Modulus	Increase in modulus of elasticity with height
Reference Height	

The linear elastic model does not account for yield strength, and the strain and stress results thus may not be realistic. Cohesion and the friction angle based on the Mohr-Coulomb failure criterion help compare the computed shear stress with the theoretical yielding stress graphically. Accordingly, in general analysis cases, the Mohr-Coulomb or other nonlinear constitutive models are recommended.

SoilWorks can simulate the variation of the modulus of elasticity with respect to height. If the increase in the modulus of elasticity with height is zero, the modulus of elasticity is constant,

If the increase is not zero, the modulus of elasticity with respect to height can be calculated as below.

$$E = E_{ref} + \left(Z_{ref} - Z\right)E_{inc} \qquad \left(Z \le Z_{ref}\right) \qquad (3.1.2)$$
$$E = E_{ref} \qquad \left(Z > Z_{ref}\right)$$

where,

E_{ref} : Modulus of elasticity (user input)

E_{inc} : Slope of increment of modulus of elasticity

Z_{ref} : Reference depth corresponding to E_{ref}

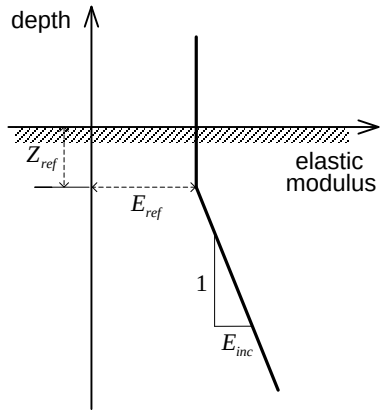

Figure 3.1.2 Schemetic daigram of variation of elastic modulus with depth

In Eq. (3.1.2), Z is the location of the integration point of the element in the finite element analysis. If the integration point is located higher than the reference height Z_{ref}, the elastic modulus may become less than zero. In order to prevent negative elastic modulus, the elastic modulus E_{ref} is used as the minimum elastic modulus.

The linear elastic model is not suitable for modeling highly nonlinear ground. It is, however, useful for modeling the structural behavior of high stiffness materials compared to soils, such as concrete and steel.

3.2 Tresca Model

3.2.1 Introduction

The Tresca model was initially developed to establish a failure criterion for metals. In geotechnical engineering, this constitutive model is widely used to model the undrained behavior of ground soil. It assumes that an object fails if the maximum shear stress at a point exceeds the limit stress, k. This criterion is numerically expressed by the following equation:

$$\frac{1}{2}\left|\sigma_3 - \sigma_1\right| = k \tag{3.2.1}$$

k represents the failure (yield) stress for pure shear when σ_3 and σ_1 are the maximum and minimum principal stresses respectively $(\sigma_1 \geq \sigma_2 \geq \sigma_3)$. The constant k is a function of hardening parameter, which is determined by tests. In order to readily use the test properties, Eq. (3.2.1) can be rewritten as,

$$\left|\sigma_3 - \sigma_1\right| = \sigma_y \tag{3.2.2}$$

where, σ_y is the uniaxial compressive strength.

3.2.2 Material Properties

The input data for the Tresca model is shown in Table 3.2.1.

Table 3.2.1: Input data for Tresca model

Input Parameters	Remarks
Yield Stress (σ_y)	Uniaxial compressive strength

3.2.3 Yield Function

Eq. (3.2.2) can be rewritten with the stress invariant J_2 and θ_0 $(0^\circ \le \theta_0 \le 60^\circ)$ as,

$$\sigma_1 - \sigma_3 = \frac{1}{\sqrt{3}}\sqrt{J_2}\left[\cos\theta_0 - \cos\left(\theta_0 + \frac{2}{3}\pi\right)\right] = \sigma_y \tag{3.2.3}$$

Rearranging Eq. (3.2.3) results in,

$$f\left(J_2, \theta_0\right) = 2\sqrt{J_2}\sin\left(\theta_0 + \frac{1}{3}\pi\right) - \sigma_y = 0 \tag{3.2.4}$$

Expressing Eq. (3.2.4) in terms of $\rho,\ \xi,\ \theta_0$,

$$f\left(\rho, \theta_0\right) = 2\rho\sin\left(\theta_0 + \frac{1}{3}\pi\right) - \sqrt{2}\sigma_y = 0 \tag{3.2.5}$$

Or, expressing in terms of $I_1,\ J_2,\ \theta\ \left(-\frac{\pi}{6} \le \theta \le \frac{\pi}{6}\right)$,

$$\begin{aligned} f\left(J_2, \theta_0\right) &= \frac{2}{\sqrt{3}}\sqrt{J_2}\left[\sin\left(\theta + \frac{2}{3}\pi\right) - \sin\left(\theta + \frac{4}{3}\pi\right)\right] - \sigma_y \\ &= 2\sqrt{J_2}\cos\theta - \sigma_y = 0 \end{aligned} \tag{3.2.6}$$

This failure criterion does not depend on the hydrostatic pressure (I_1) since the effect of hydrostatic pressure on the yield surface is not considered. The Tresca yield surface forms a prism with a regular hexagonal section (Figure 3.2.1) parallel with the hydrostatic axis in the principal stress space, and a regular hexagon on the deviatoric plane (Figure 3.2.2(a)).

A number of shortcomings exist when applying the Tresca yield criterion to the soil materials. First, it is not correct to assume that the hydrostatic pressure (or confinement pressure) does not affect the shear strength of the ground soil. Second, the Tresca yield criterion

exhibits the same failure stress in both compression and tension, whereas the tensile strength of ground soil is smaller than the compressive strength. In addition, the criterion does not account for any intermediate principal stresses.

The Tresca yield criterion can, however, simulate reasonable results when the total stress analysis is performed on saturated soil under undrained conditions, which is referred to as $\phi = 0$ analysis. According to laboratory tests, the shear strength of saturated soil under undrained conditions is independent of the hydrostatic pressure (I_1), thus enabling the use of the Tresca yield criterion. In this case, the limit stress k, which indicates the undrained shear strength, $c_u(\phi_u = 0)$, must be determined from the unconsolidated, undrained triaxial compression tests.

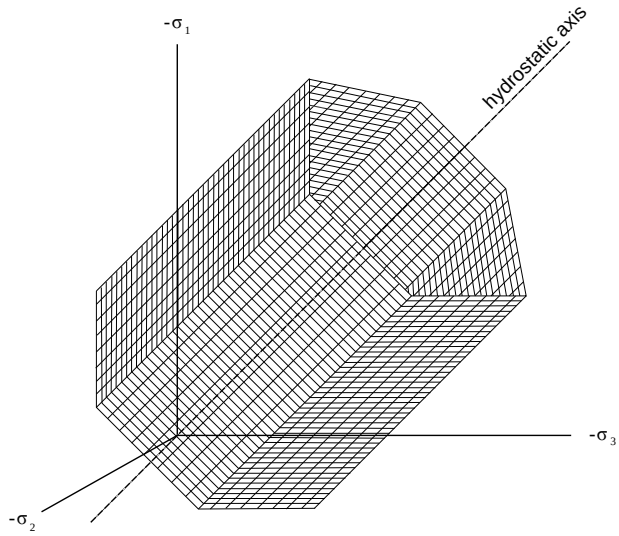

Figure 3.2.1 Shape of Tresca yield surface in the 3D space of principal stresses

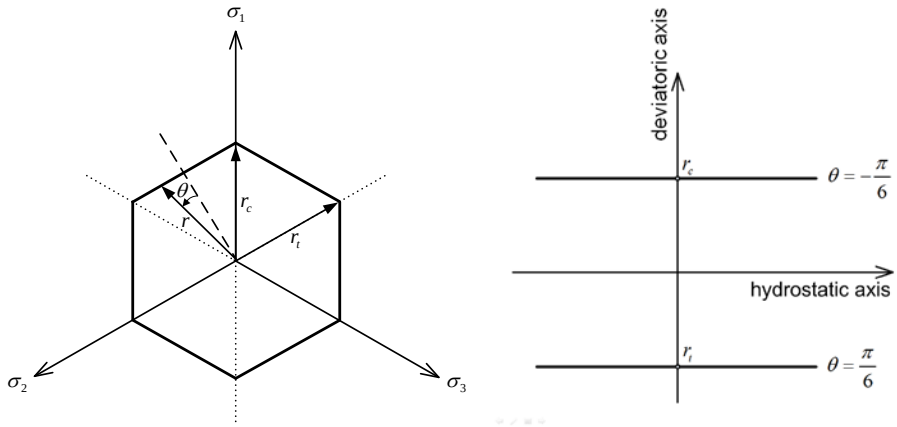

(a) Projection of yield surface on π -plane (b) Projection of yield surface on meridian plane at ($\theta = -\frac{\pi}{6}$)

Figure 3.3.2 Tresca yield surfaces on π -plane and meridian plane

3.3 von Mises Model

3.3.1 Introduction

The von Mises failure criterion states that a material fails when the octahedral shear stress (τ_{oct}) reaches a limit, which is mainly applicable to the analysis of ductile materials such as metals. In addition to its application to ground materials, it is applicable to truss, embedded truss and plate elements of steel materials such as anchors, nails and pipe piles.

3.3.2 Material Properties

The input data for the von Mises model is shown in Table 3.3.1.

Table 3.3.1 Input data for von Mises model

Input Parameters	Remarks
Yield Stress (σ_y)	Uniaxial compressive strength

3.3.3 Yield Function

The von Mises failure (yield) function is expressed using the uniaxial strength as,

$$f\left(J_2\right)=\sqrt{3J_2}-\sigma_y=0 \tag{3.3.1}$$

The von Mises failure surface forms a circular cylinder with its axis parallel to the hydrostatic axis in the principal stress space (Figure 3.3.1). If the von Mises criterion and the Tresca criterion are made coincident at compression and tensile meridian, $\rho_c(\theta_0=0^\circ)$ and $\rho_t(\theta_0=60^\circ)$, the von Mises failure surface becomes a circle circumscribing the Tresca's hexagonal yield surface on the deviatoric plane (π-plane) as shown in Figure 3.3.2 (a).

In this case, the maximum difference between the expected two failure stresses takes place

along the pure shear meridian $(\theta_0 = 30^\circ)$, and the ratio of the failure shear stress of the von Mises' criterion to that of the Tresca's criterion is $2/\sqrt{3} = 1.15$. On the other hand, if the two failure criteria are made coincident with the pure shear (the same *k* value), the von Mises' circle inscribes the Tresca's hexagonal yield surface on the π-plane as shown in Figure 3.3.2 (b). In this case, the maximum expected difference between the two failure stresses takes place along the compression meridian $\rho_c(\theta_0 = 0^\circ)$ and the tension meridian $\rho_t(\theta_0 = 60^\circ)$.

The von Mises failure criterion also retains the shortcomings like the Tresca failure criterion being applied to the soil materials in which the tension and compression strengths are equal and the shear strength is independent of the hydrostatic pressure. The von Mises yield criterion like the Tresca's, however, allows appropriate application in the case of undrained strength in saturated soil. The von Mises criterion can be conveniently used since it is free from mathematical and numerical complexities stemming from the hexagonal corners as present in the Tresca failure surface.

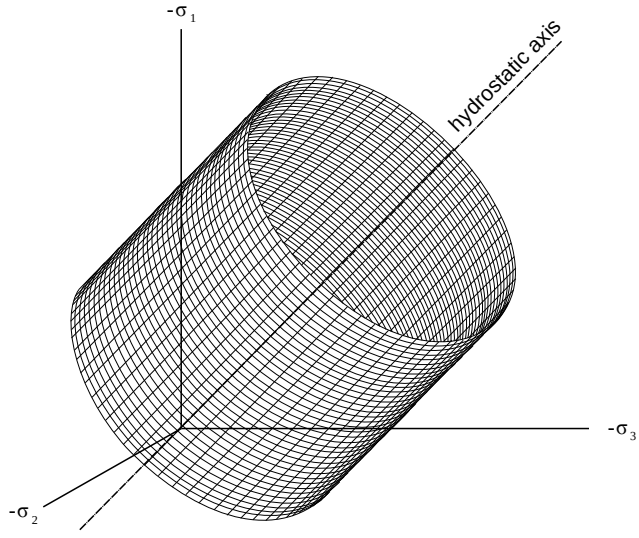

Figure 3.3.1 Shape of von Mises yield surface in the 3D space of principal stresses

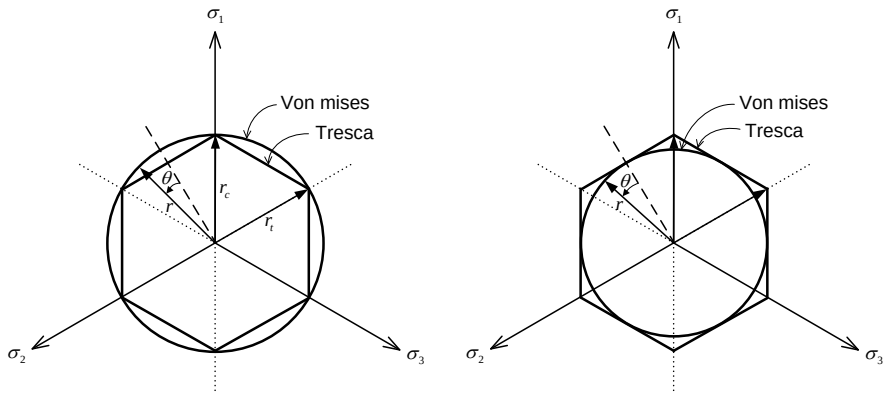

(a) In case of uniaxial stress (b) In case of pure shear stress

Projection of yield surface on π -plane

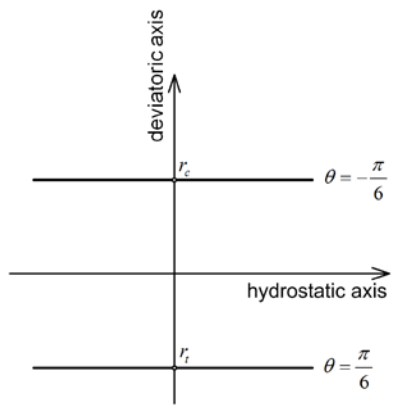

(c) Projection of yield surface on meridian plane ($\theta = -\frac{\pi}{6}$)

Figure 3.3.2 von Mises yield surfaces on π -plane and meridian plane

3.4 Mohr-Coulomb Model

3.4.1 Introduction

The Mohr-coulomb model is used to simulate the majority of ground materials. SoilWorks defines the stress-strain relationship of the model as elasto-perfectly-plastic, as shown in Figure 3.4.1(a). Such an assumption for soil behavior leads to sufficiently reliable solutions in nonlinear analysis in a general domain.

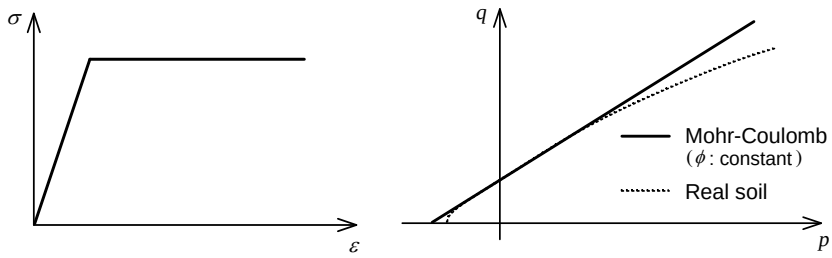

(a) Stress-strain relationship (b) Shape of yield function

Figure 3.4.1 Mohr-Coulomb model behavior and yield function

There are two main shortcomings for the Mohr-Coulomb model to be applied to soil materials. First, since the failure occurs when the largest Mohr circle is tangential to the failure envelope, the intermediate principal stress, $\sigma_2(\sigma_1 \geq \sigma_2 \geq \sigma_3)$, does not have any influence on the failure stress. This is inconsistent with experimental results. Second, the straight Mohr circle's meridian and failure envelope result in the constant strength parameter, ϕ, independent of the hydrostatic pressure (or confinement pressure) as shown in Figure 3.4.1(b). This implies that the criterion is accurate in certain limits of confinement pressure, but the accuracy diminishes with an increase in the range of confinement pressures. In addition, the discontinuous corner of the yield surface presents difficulties in numerical analysis. Also, the Mohr-Coulomb model cannot describe the compaction of soil.

Despite these limitations, the Mohr-Coulomb model has been widely and successfully used in geotechnical engineering due to the ease of application and reliable results within the practical confinement pressures.

3.4.2 Material Properties

The input data for the Mohr-Coulomb model is listed in Table 3.4.1.

Table 3.4.1 Input data for Mohr-Coulomb model

Input Parameters	Remarks
Inc. of Elastic Modulus (E_{inc})	Increase in modulus of elasticity with height
Inc. of Cohesion (c_{inc})	Increase in cohesion with height
Reference Height (y_{ref})	
Dilatancy Angle (ψ)	
Tensile Strength (σ_t)	

SoilWorks can simulate variations in elastic modulus and cohesion with respect to height using the Mohr-Coulomb model. The variation in elastic modulus is the same as explained in Section 3.1. In this section, the variation in cohesion is described. If the increase in cohesion relative to height is zero, the cohesion is constant throughout the model. In case of non-zero increment, the cohesion relative to the reference height can be calculated using the following equation.

$$\begin{aligned} c &= c_{ref} + \left(y_{ref} - y\right)c_{inc} && \left(y \le y_{ref}\right) \\ c &= c_{ref} && \left(y > y_{ref}\right) \end{aligned} \qquad (3.4.1)$$

where,

c_{ref} : Specified initial cohesion

c_{inc} : Increment of the cohesion with depth

y_{ref} : Reference depth corresponding to c_{ref}

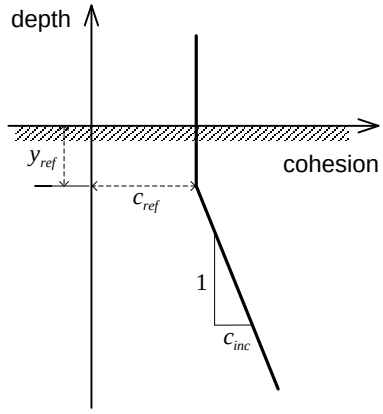

Figure 3.4.2 Schemetic diagram of variation in cohesion with respect to depth

In Eq. (3.4.1), y is the location of the integration point of the element in the finite element analysis. If the integration point is located higher than the reference height, y_{ref}, the cohesion may become less than zero. In order to prevent negative cohesion, the cohesion, c_{ref} is used as the minimum cohesion.

3.4.3 Yield Function

According to the Mohr's criterion, the failure is expressed as,

$$|\tau| = f(\sigma) \tag{3.4.2}$$

The limit shear stress (τ) on a particular plane is related to the normal stress (σ) acting on the same plane. Eq. (3.4.2) corresponds to the failure envelope of Mohr circles, and the failure envelope function, $f(\sigma)$ is determined by laboratory tests. Material failure by the Mohr's criterion takes place at the state of stress in which the largest Mohr circle is in contact with the failure envelope. This means that an intermediate principal stress, σ_2 ($\sigma_1 \geq \sigma_2 \geq \sigma_3$) does not influence the failure condition.

The simplest geometric form of the Coulomb's yield surface is a straight line, which is defined as,

$$|\tau| = c + \sigma \tan\phi \tag{3.4.3}$$

where,

c : Cohesion, vertical axis (τ) intercept of the failure envelope

ϕ : Internal friction angle, slope of the failure envelope

The failure criterion defined by Eq. (3.4.3) is referred to as the Mohr-Coulomb failure criterion. Because of its accuracy and simplicity, this has been the most widely used ground material.

Expressing the Mohr-Coulomb equation in terms of the principal stresses $(\sigma_1 \geq \sigma_2 \geq \sigma_3)$, Eq (3.4.3) can be converted into,

$$\sigma_1 \frac{(1-\sin\phi)}{2c\cos\phi} - \sigma_3 \frac{(1+\sin\phi)}{2c\cos\phi} = 1 \tag{3.4.4}$$

Eq. (3.4.3) can also be expressed using the stress invariants I_1 and J_2 and θ as,

$$f(I_1, J_2, \theta) = -\frac{1}{3} I_1 \sin\phi + \sqrt{J_2}\left(\cos\theta + \frac{1}{\sqrt{3}}\sin\theta\sin\phi\right) - c\cos\phi = 0 \tag{3.4.5}$$

Expressing Eq. (3.4.3) in terms of invariants, ξ, ρ and θ_0, the equation becomes,

$$\begin{aligned} f(\xi, \rho, \theta_0) = &-\sqrt{2}\xi\sin\phi + \sqrt{3}\rho\sin\left(\theta_0 + \frac{\pi}{3}\right) \\ &- \rho\cos\left(\theta_0 + \frac{\pi}{3}\right)\sin\phi - \sqrt{6}c\cos\phi = 0 \end{aligned} \tag{3.4.6}$$

The plastic potential function can be expressed using the format of Eq. (3.4.5) as,

$$g(I_1, J_2, \theta) = -\frac{1}{3} I_1 \sin\psi + \sqrt{J_2}\left(\cos\theta + \frac{1}{\sqrt{3}}\sin\theta\sin\psi\right) - c\cos\psi = 0 \qquad (3.4.7)$$

The Mohr-Coulomb failure surface forms an irregular hexagonal pyramid in the 3D principal stress space in which its meridian is a straight line, and the failure surface becomes an irregular hexagon on the π plane $(\sigma_1 + \sigma_2 + \sigma_3 = 0)$. In order to define the irregular hexagon, the lengths of ρ_{t0} and ρ_{c0} are required, which are calculated by substituting the conditions of $(\xi = 0, \rho = \rho_{t0}, \theta_0 = 60^\circ)$ and $(\xi = 0, \rho = \rho_{c0}, \theta_0 = 0^\circ)$ into Eq. (3.4.6).

$$\rho_{t0} = \frac{2\sqrt{6}c\cos\phi}{3 + \sin\phi} \qquad (3.4.8)$$

$$\rho_{c0} = \frac{2\sqrt{6}c\cos\phi}{3 - \sin\phi} \qquad (3.4.9)$$

From Eq. (3.4.8) and Eq. (3.4.9), ρ_{t0} / ρ_{c0} is obtained.

$$\frac{\rho_{t0}}{\rho_{c0}} = \frac{3 - \sin\phi}{3 + \sin\phi} \qquad (3.4.10)$$

Since the Mohr-Coulomb failure surfaces geometrically form the identical shape on deviatoric planes (i.e, for different values of I_1 or ξ), the ratio of ρ_t / ρ_c on any deviatoric plane remains constant.

$$\frac{\rho_t}{\rho_c} = \frac{\rho_{t0}}{\rho_{c0}} = \frac{3 - \sin\phi}{3 + \sin\phi} \qquad (3.4.11)$$

The principal tension stresses in the Mohr-Coulomb model are limited not to exceed a given tensile strength. Such limitation of tension zone is called a Tension-cutoff. SoilWorks provides this tensile limitation based on the Rankine's yield criterion, which states that the failure occurs when the maximum principal stress reaches the tensile stress, used in combination with the Mohr-Coulomb model.

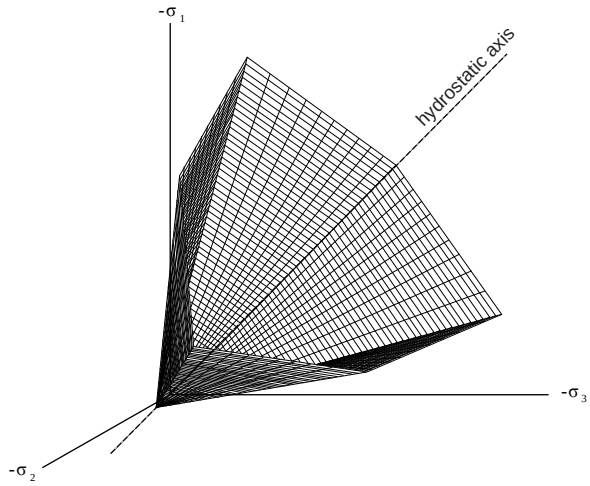

Figure 3.4.3 Mohr-Coulomb yield surface in 3D principal stress space

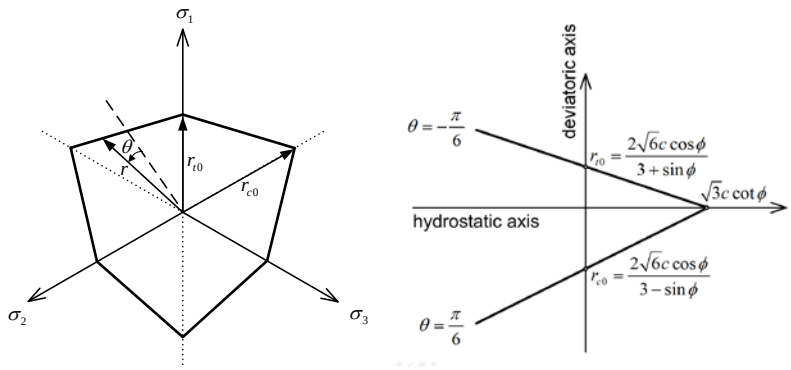

(a) Projection of yield surface on π -plane (b) Projection of yield surface on meridian plane ($\theta = -\frac{\pi}{6}$)

Figure 3.4.4 Mohr-Coulomb yield surfaces on π -plane and meridian plane

3.5 Drucker-Prager Model

3.5.1 Introduction

The Drucker-Prager model was introduced to resolve the numerical problems encountered at the corners of the Mohr-Coulomb yield surface. The Drucker-Prager model is essentially an extension of the von Mises model, obtained by defining the deviatoric stresses as a function of hydrostatic pressure. It is widely used in practice and is also known as the extended von Mises criterion.

3.5.2 Material Properties

The input data for the Drucker-Prager model is listed in Table 3.5.1.

Table 3.5.1 Input data for Drucker-Prager model

Input Parameters	Remarks
Inc. of Elastic Modulus (E_{inc})	Increase in modulus of elasticity
Inc. of Cohesion (c_{inc})	Increase in cohesion
Reference Height (y_{ref})	

The Drucker-Prager model can consider variations in elastic modulus and cohesion with respect to height like the Mohr-Coulomb model. Its internal algorithm is identical to that of the Mohr-Coulomb model.

3.5.3 Yield Function

The Drucker-Prager failure (yield) criterion can be expressed using the stress invariants I_1 and J_2 as,

$$f\left(I_1, J_2\right) = \sqrt{J_2} - \alpha I_1 - k = 0 \qquad (3.5.1)$$

or using the the relationships, $\xi = I_1 / \sqrt{3}$ and $\rho = \sqrt{2J_2}$

$$f(\xi, \rho) = \rho - \sqrt{6}\alpha\xi - \sqrt{2}k = 0 \qquad (3.5.2)$$

The material constants, α and k, are determined from experiments, which can be expressed in terms of cohesion, c and internal friction angle, ϕ of the Mohr-Coulomb criterion by coinciding the state of stresses. If α is zero in Eq. (3.5.2), the Drucker-Prager failure criterion becomes identical to the von Mises failure criterion.

Figure 3.5.1 shows the Drucker-Prager failure surface in 3D principal stress space. The failure surface retains the form of a regular cone with the axis of the hydrostatic pressure ($\sigma_1 = \sigma_2 = \sigma_3$). The failure surface can be considered as a smoothened Mohr-Coulomb failure surface or as the extension of the von Mises failure surface for hydrostatic pressure-dependent materials like soils.

The advantages of using the Drucker-Prager model are as follows:

- ✓ The failure criterion contains only two material parameters, α and k leading to a simple failure criterion, which can be easily determined by conventional tri-axial compression tests.
- ✓ The failure surface is smooth, which renders mathematical convenience even in the applications to 3D analysis.
- ✓ Unlike the von Mises model, the model accounts for the effect of the hydrostatic pressure on the failure surface.
- ✓ Since the yield surface is a straight line on the meridian plane, the model is especially useful even when the curvature of the material's failure envelope is ignored.

The relationship between the material parameters of the Drucker-Prager and the Mohr-Coulomb failure criteria is described below:

There are several ways to make the Mohr-Coulomb hexagonal failure surface compatible with the Drucker-Prager cone. When the vertices of the two surfaces are made coincident with each other along the spatial diagonal line, only one additional compatible condition is necessary for adjusting the size of the Drucker-Prager cone. For example, if the two

surfaces are made coincident along the compressive meridian ρ_c in which $\theta_0 = 0^\circ$, the relationships of the material parameters (α, k and c, ϕ) can be expressed as follows:

$$\alpha = \frac{2\sin\phi}{\sqrt{3}(3-\sin\phi)}, \qquad k = \frac{6c\cos\phi}{\sqrt{3}(3-\sin\phi)} \tag{3.5.3}$$

The cone corresponding to the parameters in Eq. (3.5.3) circumscribes the hexagonal pyramid, and it represents the outer boundary of the Mohr-Coulomb failure surface. On the other hand, the material parameters of the inscribed cone passing through the tensile meridian, ρ_t in which $\theta_0 = 60^\circ$, can be defined using Eq. (3.5.4).

$$\alpha = \frac{2\sin\phi}{\sqrt{3}(3+\sin\phi)}, \qquad k = \frac{6c\cos\phi}{\sqrt{3}(3+\sin\phi)} \tag{3.5.4}$$

The relationships of the parameters like the above can be also obtained for other cases, but are rarely useful. As an example of plain strain however, the Drucker-Prager and Mohr-Coulomb criteria are expected to show an identical yielding load (or plastic failure load) for a bearing capacity problem (Chen, 1975). In order to determine the parameters, α and k in such a case, the following two conditions need to be used:

- ✓ Plane strain deformation condition
- ✓ Identical rate of dissipation of mechanical energy per unit volume

Based on the above two conditions, the relationships between the material parameters can be formulated (Drucker and Prager, 1952).

$$\alpha = \frac{\tan\phi}{\left(9+12\tan^2\phi\right)^{1/2}}, \qquad k = \frac{3c}{\left(9+12\tan^2\phi\right)^{1/2}} \tag{3.5.5}$$

In case of plane strain, using the relationship in Eq. (3.5.5) converts the failure criterion of Eq. (3.5.1) to Eq. (3.4.3) of the Mohr-Coulomb model.

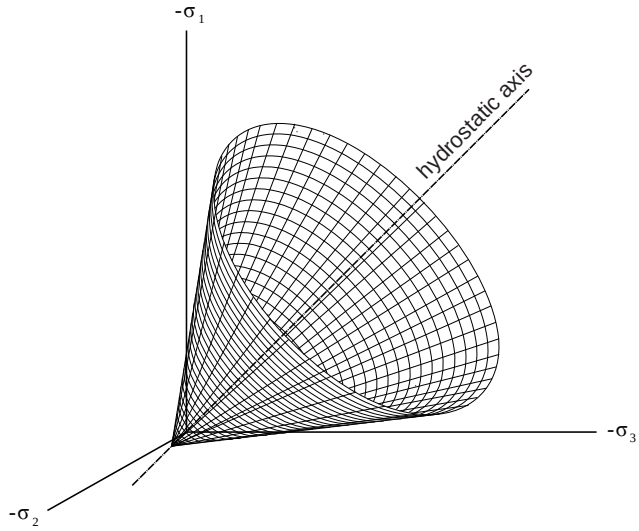

Figure 3.5.1 Drucker-Prager yield surface in 3D principal stress space

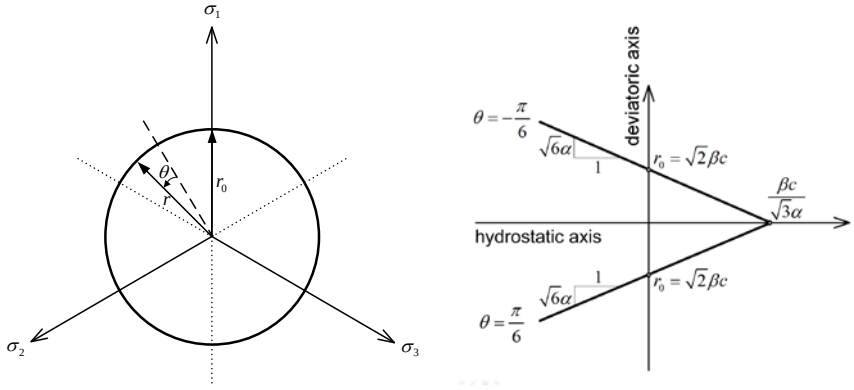

(a) Yield surface on π -plane (b) Yield surface on meridian plane

Figure 3.5.2 Drucker-Prager yield surfaces on π -plane and meridian plane

3.6 Hyperbolic Model (Duncan-Chang Model)

3.6.1 Introduction

The stress-strain relationship for soil becomes nonlinear as it approaches close to failure. A nonlinear elastic model simulates such a ground behavior by changing the soil parameters. SoilWorks uses the equation suggested by Duncan and Chang (1970) to determine the soil parameters. In this equation, the stress-strain curve is defined as a hyperbolic function. The soil parameters are a function of the confinement stress and shear stress. This nonlinear material model is very useful because it can be defined only by the soil parameters, which can be easily obtained from triaxial tests or from the literatures.

The nonlinear stress-strain curve of Duncan and Chang is expressed as a hyperbolic curve in the relationship of the shear stress $(\sigma_1 - \sigma_3)$ and axial strain. Depending on the state and path of the stress, three soil parameters are required, which are initial modulus of elasticity (E_{init}), tangential modulus of elasticity (E_{tan}) and unloading-reloading modulus of elasticity (E_{ul}) as shown in Figure 3.6.1.

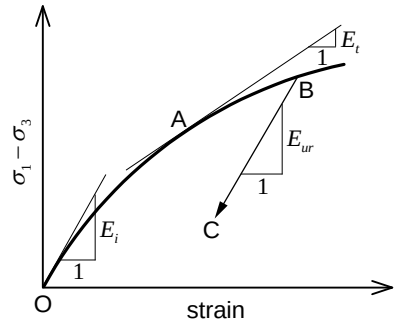

Figure 3.6.1 Nonlinear stress-strain relationship

3.6.2 Material Properties

The input data for the hyperbolic model is listed in Table 3.6.1.

Table 3.6.1 Input data for hyperbolic model

Input Parameters	Remarks
Poisson's Ratio (ν)	Constant used when K_b = 0
Cohesion (c)	
Internal Friction Angle (ϕ)	
Initial Loading Modulus (K)	
Exponent (n)	Exponent for initial stiffness
Failure Ratio (R_f)	
K_{ur}	Unloading-reloading modulus
K_b	Bulk modulus number
Exponent (m)	Exponent for bulk modulus
Min. Tangential Modulus	
Min. Confinement Stress ($\sigma_{\min}$)	
Atmospheric Pressure(P_a)	

The material parameters and exponents for a nonlinear model can be expressed by plotting the triaxial test results on a log vs log graph as shown in Figure 3.6.2. The values of stiffness, E / p_a and B_m / p_a, can be calculated from Eq. (3.6.1 & 3.6.2). These results are plotted against σ_3 / p_a in Figure 3.6.2. The initial loading modulus, K can be obtained from the graph at $\sigma_3 / p_a = 1$ with the vertical axis representing E / p_a. The slopes, n and m, from the straight lines connecting the results are the exponents that define the influence of confinement stress.

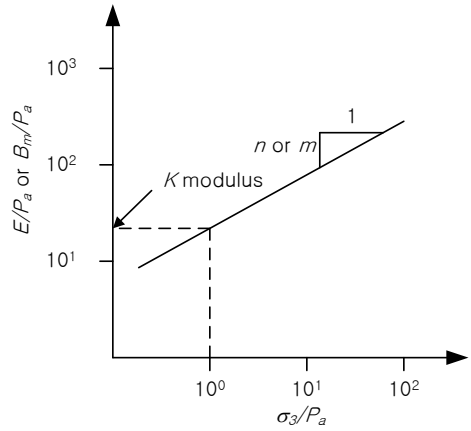

Figure 3.6.2 Properties of nonlinear ground material model

The bulk modulus, B_m, is defined as follows:

$$B_m = \frac{(\Delta\sigma_1 + \Delta\sigma_2 + \Delta\sigma_3)/3}{\Delta\varepsilon_v} \tag{3.6.1}$$

where,

$\Delta\sigma$: Change in principal stress

$\Delta\varepsilon_v$: Change in volumetric strain

3.6.3 Initial Modulus

When the ground is subjected to no shear stress (i.e., $\sigma_1 - \sigma_3 = 0$), the stress-strain behavior can be modeled using the initial elastic modulus, E_i. This initial modulus is controlled by the confinement stress, σ_3, which is expressed as,

$$E_i = K_L p_a \left(\frac{\sigma_3}{p_a}\right)^n \tag{3.6.2}$$

where,

E_i : Initial modulus, which is a function of confinement stress

K_L : Loading coefficient

p_a : Atmospheric pressure (a factor used for normalization)

σ_3 : Confinement pressure

n : Exponent to define the influence of confinement pressure for the initial modulus (range of values: 0-1)

If n is equal to 1.0, the initial modulus, E_i is directly proportional to the confinement stress. If it is zero, the initial modulus is independent of the confinement stress.

If the confinement stress is zero or negative, the initial modulus can also become a zero or negative value. In order to prevent such a problem from happening, SoilWorks sets a minimum value for the confinement stress to 0.01 p_a.

3.6.4 Tangential Modulus

Soil is known to follow a loading path once it becomes subjected to a shear stress greater than a precedent load. When the soil follows the loading path, its constitutive behavior is governed by the tangential modulus, E_t. This modulus in the Duncan and Chang model is defined as a function of material property, triaxial deviatoric stress $(\sigma_1 - \sigma_3)$ and confinement stress (σ_3).

$$E_t = \left[1 - \frac{R_f(\sigma_1 - \sigma_3)(1 - \sin\phi)}{2c\cos\phi + 2\sigma_3 \sin\phi}\right]^2 E_i \qquad (3.6.3)$$

where,

E_t : Tangential modulus

E_i : Initial tangential modulus

ϕ : Internal friction angle

c : Cohesion

R_f : Failure ratio between the asymptotic curve of a parabolic curve and the maximum shear strength (range of values: 0.75-1)

The minimum value of E_t is set to p_a. If this value is too small, it may cause convergence problems.

3.6.5 Unloading-Reloading Modulus

When the ground is unloaded from the state of a very large shear stress, a nonlinear model uses the unloading- reloading modulus, E_{ur}. The unloading-reloading modulus is calculated by a method as used for the initial modulus, except that the unloading-reloading modulus number, K_{ur} is used instead of K_L. Therefore, its equation is defined as,

$$E_{ur} = K_{ur} p_a \left(\frac{\sigma_3}{p_a} \right)^n \tag{3.6.4}$$

Unlike the tangential modulus, the unloading-reloading modulus, E_{ur}, is independent of the level of shear stress. If the unloading-reloading modulus number, K_{ur} is not specified, K_{ur} is defined as the loading modulus number, K_L.

3.6.6 Poisson's Ratio

The Poisson's ratio of a nonlinear elastic model can be defined as a constant irrespective of the state of stress or can be calculated from the bulk modulus of the ground depending on the confinement stress. In the case of the latter, the bulk modulus is defined using the following equation:

$$B_m = K_b p_a \left(\frac{\sigma_3}{p_a} \right)^m \tag{3.6.5}$$

where,

B_m : Bulk modulus

K_b : Bulk modulus number (range of values: 200-700)

m : Bulk modulus exponent (range of values: 0-1)

The relationship of the bulk modulus to the Poisson's ratio can be expressed based on the elastic theory as,

$$B_m = \frac{E}{3(1-2\nu)} \tag{3.6.6}$$

From the Eq. (3.6.6), if the Poisson's ratio is zero, $B_m = E/3$. If Poisson's ratio is 0.49, $B_m = 16.67E$. It is recommended that a Poisson's ratio in the range between 0 and 0.49 be used.

3.6.7 Yielding Zone

The yielding condition for a nonlinear elastic model cannot be defined. However, a yielding zone of satisfying the following criterion can be defined in order to show the zone of large shear stress.

$$\frac{\sigma_1 - \sigma_3}{2} - \frac{\sigma_1 + \sigma_3}{2}\sin\phi \geq R_f c\cos\phi \tag{3.6.7}$$

The failure ratio, R_f in the Duncan and Chang equation is used as Eq. (3.6.8).

$$(\sigma_1 - \sigma_3)_f = R_f(\sigma_1 - \sigma_3)_{ult} \tag{3.6.8}$$

The ultimate strength term, $(\sigma_1 - \sigma_3)_{ult}$, represents the asymptotic curve in which the hyperbolic stress-strain curve approaches to large strains. Also $(\sigma_1 - \sigma_3)_f$ is the deviatoric stress at failure.

The following condition is obtained from the Mohr circle:

$$\frac{(\sigma_1 - \sigma_3)_{ult}}{2} - \frac{(\sigma_1 + \sigma_3)_{ult}}{2}\sin\phi = c\cos\phi \tag{3.6.9}$$

Substituting Eq. (3.6.8) into Eq. (3.6.9), Eq. (3.6.10) can be derived.

$$\frac{(\sigma_1 - \sigma_3)_f}{2} - \frac{(\sigma_1 + \sigma_3)_f}{2}\sin\phi = R_f c\cos\phi \tag{3.6.10}$$

Comparing the two equations, Eq. (3.6.7) and Eq. (3.6.10), the inequality equation can be said to provide an index of how close the state of stress is to the state of failure.

3.7 Hoek-Brown Model

3.7.1 Introduction

Hoek and Brown (1980) proposed a concept of equivalent continuum for defining the effect of stress reduction due to the failure of a jointed rock mass. A failure function was proposed to distinguish intact rock and broken rock. Once the rock failure is defined by the failure function, specific coefficients defining the failure function are reduced to simulate the stress reduction phenomenon. The method proposed by Hoek and Brown defines the uniaxial compression strength of rock, which cannot be considered by the Mohr-Coulomb method. This advantage led to a wide use of the Hoek-Brown model in accurately reflecting the behavior of rock.

3.7.2 Material Properties

The input data for the Hoek-Brown model is listed in Table 3.7.1.

Table 3.7.1 Input data for Hoek-Brown model

Input Parameters	Remarks
Initial m	Initial m at the intact state
Initial s	Initial s at the intact state
Residual m	m at the broken state
Residual s	s at the broken state
Uniaxial Compression Strength	

3.7.3 Yield Function

A commonly used failure criterion in rock mechanics is Hoek-Brown failure criterion (Eq. (3.7.1), which ignores the intermediate principal stress.

$$\sigma_1 = \sigma_3 + \sqrt{m\sigma_c\sigma_3 + s\sigma_c^2} \tag{3.7.1}$$

where, σ_c represents the unconfined uniaxial compressive strength, and *m* and *s* are empirical parameters indicating the extent of breakage of the rock mass.

For the convenience of elasto-plastic finite element calculations, Eq. (3.7.2) is expressed using the stress invariants.

$$F_{HB} = 4J_2\cos^2\theta + m\sigma_c\sqrt{2}\left(\frac{\sin\theta}{\sqrt{3}} + \cos\theta\right) + m\sigma_c\frac{I_1}{3} - s\sigma_c^2 = 0 \qquad (3.7.2)$$

I_1 is the first stress invariant; J_2 is the second deviatoric stress invariant; and σ_c is the uniaxial compressive strength of the rock mass.

The Hoek-Brown model retains the shape of a pointed bullet gradually enlarging along the hydrostatic axis in the space of principal stresses. The deviatoric plane shape shows a hexagonal shape consisted of 6 parabolic surfaces. This shape causes undesirable singularity at the vertex where the surfaces meet and the gradient is non-unique. In order to mitigate any singularities, an elliptical function is used to describe the variation of the trace of the surface in the deviatoric planes for a sextant of the stress space, i.e., $-\pi/6 \le \theta \le \pi/6$. SoilWorks uses the modified Hoek-Brown criterion proposed by Wan (1994).

$$F = q^2 g^2(\theta) + \sigma_c^* q g(\theta) + 3\sigma_c^* p - s\sigma_c^2 = 0 \qquad (3.7.3)$$

where, $\sigma_c^* = m\sigma_c/3$, $q = \sqrt{3J_2}$, $p = I_1/3$ and the expression for deviatoric plane shape, $g(\theta)$ is given by,

$$g(\theta) = \frac{4(1-e^2)\cos^2(\pi/6+\theta) + (1-2e)^2}{2(1-e^2)\cos^2(\pi/6+\theta) + (2e-1)D} \qquad (3.7.4)$$

where,

$$D = \sqrt{4(1-e^2)\cos^2(\pi/6+\theta) + 5e^2 - 4e}$$

Figure 3.7.1 shows the Hoek-Brown yield surface in the principal stress space.

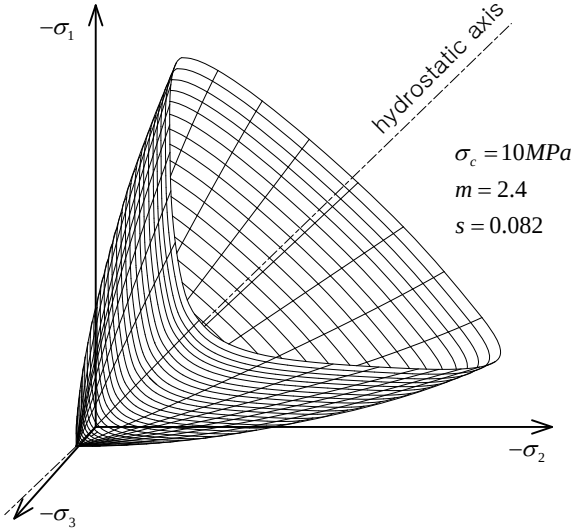

Figure 3.7.1 Hoek-Brown failure surface

3.8 Modified Cam-Clay Model

3.8.1 Introduction

The Modified Cam-clay model is a critical state model while being an elasto-plastic hardening material model. The model was numerically formulated on the bases of Atkinson and Brandsby (1978) and Britto and Gunn (1987). The stresses used to formulate the Modified Cam-clay model are not the total but all effective stress factors.

Figure 3.8.1(a) shows the relationship between the pressure and the change in general ground volume, which includes both normal consolidation and over-consolidation. The over-consolidation line is also known as the "swelling" line, which considers the state of stress during the over-consolidated stage. The applied stress increases along the over-consolidation line moving onto the normal consolidation line. Once it crosses the intersection of the two lines, additional increase in stress is represented by the state of stress following down the normal consolidation line.

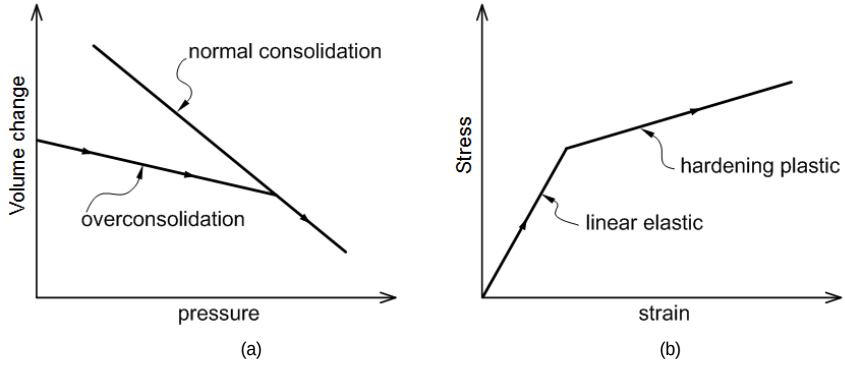

Figure 3.8.1 Similarity between volume change vs. pressure and stress vs. strain

Figure 3.8.1 shows similarity between the graph of volume change vs. pressure and the graph of stress-strain relationship. If Figure 3.8.1(a) is rotated counter-clockwise by 90 degrees, it becomes similar to Figure 3.8.1(b) of the characteristics of the elastic-hardening plastic stress-strain curve. That is, the over-consolidation line resembles the initial linear elastic zone, while the normal consolidation line resembles the hardening plastic zone of the stress-strain relationship.

3.8.2 Material Properties

The input data for the Modified Cam-Clay model is listed in Table 3.8.1.

Table 3.8.1Input data for Modified Cam-clay model

Input Parameters	Remarks
Over Consolidation Ratio (OCR)	The highest stress experienced divided by the current stress
Slope of Consol. Line (λ)	Slope of normal consolidation line
Slope of Over Consol. Line (κ)	Slope of over-consolidation line
Pre-Consolidation Void Ratio (e_c)	Pre-Consolidation void ratio
Critical State Specific Vol. (Γ)	Specific volume at p' =1
Slope of Critical State Line (M)	Slope of critical state line
Pre-Consolidation Load (p'_c)	Pre-consolidation pressure
Pre-Consolidation Vertical Stress (σ_c)	Pre-consolidation vertical stress

The over-consolidation ratio, OCR, above can be obtained from site investigation results, literatures, measured data and analysis of precedence of adjacent design. Under normal consolidation, OCR is set to 1.

The material properties, $\lambda, \kappa, \Gamma, M$ listed in Table 3.8.1 can be further explained in Figure 3.8.2. Especially M can be defined by straight line slope of the critical state line (Figure 3.8.2(a)) projected onto the $p'-q$ plane as in Figure 3.8.2(b).

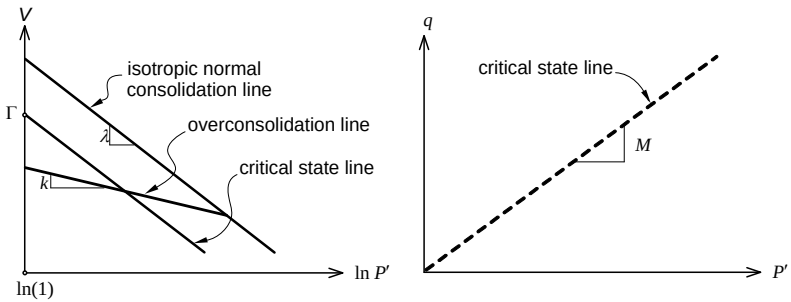

(a) Virgin and over-consolidation curves (b) Critical state line

Figure 3.8.2. Modified Cam-clay model material property definition

The relationship of the compression versus vertical pressure of soil can be generally obtained from one dimensional consolidation tests. From the graph of $\log_{10}(p)$ versus void ratio (e), the compression index (C_c) and the recompression index (C_s) can be generally obtained. The compression index and the recompression index are related to λ & κ by the following equations:

$$\lambda = \frac{C_c}{2.303}$$
$$\kappa = \frac{C_s}{2.303} \qquad (3.8.1)$$

In addition, λ and κ can be estimated from the graph of the void ratio versus $\ln(p)$ instead of the graph of the void ratio versus $\log_{10}(p)$.

Since the Modified Cam-Clay model was formulated on the basis of the unit, kN-m, the same unit must be used for compression and recompression index calculations. The same unit is also recommended for the unit setting in the program.

The factor, N can be estimated by projecting the normal consolidation line onto the vertical line of p =1.0 of the graph of V vs. $\ln(p)$. Once N is calculated, the critical state specific volume, Γ can be obtained by Eq. (3.8.2).

$$\Gamma = N - (\lambda - \kappa)\ln 2 \qquad (3.8.2)$$

The parameter Γ is defined by the intersection of the critical state line and the function line with $p = 1.0$ as shown in Figure 3.8.2(a).

From test data, e-logP curve is computed as shown in following figure. The pre-consolidation state means the inflection point has pre-consolidation void ratio(e_c) and pre-consolidation pressure (p_c) in the figure below.

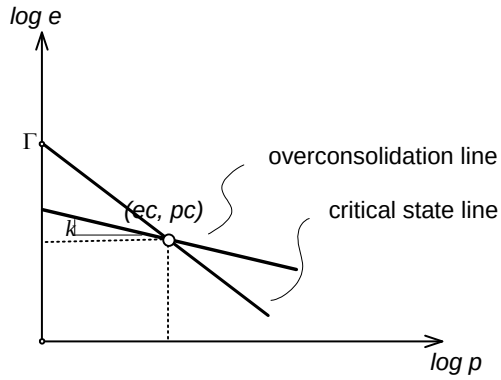

Figure 3.8.3 Graph of Pre-Consolidation State

The critical state specific volume and the pre-consolidation specific volume is represented by using pre-consolidation void ratio.

$$\Gamma_c = 1 - e_c \tag{3.8.3}$$

The slope of the critical state line, M , can be estimated by the relationship of the effective shear resistance angle (obtained by drainage tests), where ϕ' is the effective internal friction angle of the effective stress concept obtained from triaxial compression tests.

$$M = \frac{6\sin\phi'}{3-\sin\phi'} \tag{3.8.4}$$

In SoilWorks, the pre-consolidation pressure, p'_c can be automatically calculated by the program, specified by the user or computed by critical state stress. The auto-calculation method is explained in Eq. (3.8.17) in detail. The user defined value must be equal to or greater than the value of Eq. (3.8.17) to secure convergence in numerical analysis.

In order to use the Modified Cam-Clay model, other important data are required, which are the state of the present (initial) soil stress and the initial yield surface. Composing the state of the initial soil stress is relatively simple, which can be obtained using the same procedures as for other nonlinear analyses. The initial yield surface can be defined by specifying the pre-consolidation pressure, p'_c , or by calculating p'_c from the initial in-situ

stresses with the over-consolidation ratio (OCR). Refer to Chapter 3.8.4 for details.

3.8.3 Yield Function

The yield function of the Modified Cam-clay model is shown in Figure 3.8.3.

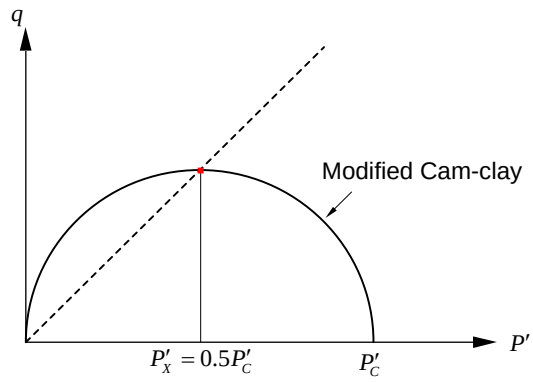

Figure 3.8.4 Yield function of Modified Cam-clay model

The yield function of the Modified Cam-Clay model is given by Britto and Gunn, 1987 (Eq. 3.8.5).

$$q^2 = M^2 p' p'_c - M^2 p'^2 \qquad (3.8.5)$$

where, p'_c is pre-consolidation pressure.

The peak mean stress (p'_x) is used to determine the magnitude of the yield surface for the Modified Cam-clay model. The peak mean stress is the isotropic pressure when the ground reaches the critical state as shown in Figure 3.8.4. The shear stress, q at the critical state is given by Eq. (3.8.6).

$$q = Mp'_x \qquad (3.8.6)$$

Substituting the value (q) into the yield function results in Eq. (3.8.7).

$$p'_c = 2p'_x \tag{3.8.7}$$

Therefore, the yield function, F for the Modified Cam-clay model can be written as,

$$F = \frac{q^2}{p'} + M^2 p' - 2M^2 p'_x \tag{3.8.8}$$

where,

$$p' = \frac{I'_1}{3}$$
$$q = \sqrt{3J_2} \tag{3.8.9}$$

The equations representing the over-consolidation line and the critical state line can be used to determine the peak mean stress (p'_x). As shown in Figure 3.8.4, the specific volume (V_x) at the critical state with respect to a specific over-consolidation line can be written as Eq. (3.8.10).

$$V_x = V_0 + \kappa \ln p'_0 - \kappa \ln p'_x \tag{3.8.10}$$

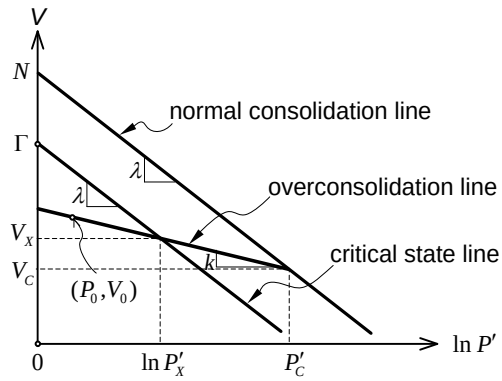

Figure 3.8.5 Definition of ground properties for Modified Cam-clay model

The specific volume, V_x , can be calculated from the critical state line.

$$V_x = \Gamma - \lambda \ln p'_x \tag{3.8.11}$$

Eliminating the specific volume term, V_x from the above two equations, an equation for the peak mean stress, p'_x is derived as Eq. (3.8.12).

$$p'_x = \exp\left(\frac{\Gamma - V_0 - \kappa \ln p'}{\lambda - \kappa}\right) \tag{3.8.12}$$

3.8.4 Initial Condition

The initial ground condition together with the initial stress is defined by the initial specific volume, V_0. The initial stress must be defined in an analysis with the Modified Cam-clay material model. In order to calculate V_0, the initial pre-consolidation pressure (p'_c) must be known. The relationship between the initial specific volume and the pre-consolidation pressure is illustrated in Figure 3.8.5.

SoilWorks provides two methods of defining the pre-consolidation pressure, p'_c, either user-defined or auto-calculated by the program. SoilWorks can automatically calculate the pre-consolidation pressure from the in-situ stresses, over-consolidation ratio (OCR), and the lateral earth pressure coefficient at rest (K_0). If the pre-consolidation pressure is undefined, the following procedure is used to estimate the pre-consolidation pressure. The initial stress in Modified Cam-clay model analysis means the current initial stress state, which is given by Eq. (3.8.13).

$$\{\sigma'_0\} = \begin{Bmatrix} \sigma'_{X0} \\ \sigma'_{Y0} \\ \sigma'_{Z0} \\ \tau_{XY0} \end{Bmatrix} \tag{3.8.13}$$

The maximum vertical stress that the ground has ever experienced can be usually determined by Oedometer tests. The over-consolidation ratio (OCR) is defined as the ratio of the highest vertical stress in the past ($\sigma'_{v\max}$) to the current vertical stress (σ'_v). The user defines the OCR depending on the type of ground. The relationship between the maximum vertical stress, $\sigma'_{v\max}$ and the maximum lateral stress, $\sigma'_{h\max}$ is approximated using the lateral earth pressure coefficient (K_0).

$$\begin{aligned} K_0 &= 1 - \sin\phi' \\ \sigma'_{h\max} &= K_0 \sigma'_{v\max} \end{aligned} \tag{3.8.14}$$

If the shear stress is assumed to be zero, the maximum stress vector ($\sigma'_{\max}$) can be written as Eq. (3.8.15).

$$\boldsymbol{\sigma}'_{\max} = \begin{Bmatrix} \sigma'_{X\max} \\ \sigma'_{Y\max} \\ \sigma'_{Z\max} \\ 0 \end{Bmatrix} = \begin{Bmatrix} \sigma'_{Y0} K_0 (\mathrm{OCR}) \\ \sigma'_{Y0} (\mathrm{OCR}) \\ \sigma'_{Y0} K_0 (\mathrm{OCR}) \\ 0 \end{Bmatrix} \tag{3.8.15}$$

The historical peak mean stress, $p'_{\max}$ and maximum shear stress, $q_{\max}$ are as follows:

$$\begin{aligned} p'_m &= \frac{1}{3}\left(\sigma'_{x\max} + \sigma'_{y\max} + \sigma'_{z\max}\right) \\ q'_m &= \frac{1}{\sqrt{2}}\sqrt{\left(\sigma'_{x\max} - \sigma'_{y\max}\right)^2 + \left(\sigma'_{y\max} - \sigma'_{z\max}\right)^2 + \left(\sigma'_{z\max} - \sigma'_{x\max}\right)^2} \end{aligned} \tag{3.8.16}$$

The pre-consolidation pressure, p'_c can be determined by substituting Eq. (3.8.16) into the yield function Eq. (3.8.5) of the Modified Cam-clay model.

$$p'_c = \frac{1}{M^2 p^2_{\max}}\left(q^2_{\max} + M^2 p^2_{\max}\right) \tag{3.8.17}$$

Once the pre-consolidation pressure, p'_c is defined by the user or calculated by Eq. (3.8.17), the initial specific volume (V_0) can be determined. First, the intersection of the normal consolidation line, N and the vertical axis (i.e., point at $\ln p' = 0$) is obtained by

Eq. (3.8.18).

$$N = \Gamma + \left(\lambda - \kappa\right)\ln 2 \tag{3.8.18}$$

Next, the specific volume at the critical state can be found from the normal consolidation line passing through the pre-consolidation pressure, p'_c.

$$v_c = N - \lambda \ln p'_c \tag{3.8.19}$$

Also, the initial specific volume, V_0 can be expressed as Eq. (3.8.20) from the over-consolidation line passing through the pre-consolidation pressure, p'_c.

$$v_0 = v_c + \kappa \ln\left(\frac{p'_c}{p'_0}\right) \tag{3.8.20}$$

From this equation, the initial mean stress (p'_0) can be obtained from the initial stress using Eq. (3.8.21).

$$p'_0 = \frac{1}{3}\left(\sigma'_{x0} + \sigma'_{y0} + \sigma'_{z0}\right) \tag{3.8.21}$$

3.9 Sekiguchi-Ohta Model

3.9.1 Introduction

The Sekiguchi-Ohta (1977)[1] model is an extended model of the Ohta (1971)[2] model on the basis of the dilatancy theory proposed by Shibata (1963)[3]. This model together with the Cam-Clay model is a representative cohesive soil model that can consider not only the elasto-plastic but also the elasto-viscoplastic behavior. Both models can be used in consolidation analysis. In addition, this model can be combined with other material models and elements in SoilWorks.

3.9.2 Material Properties

3.9.2.1 Elasto-plastic Material Properties

The input data required to define the elasto-plastic behavior of the Sekiguchi-Ohta model is listed in Table 3.9.1.

Table 3.9.1 Elasto-plastic material properties for Sekiguchi-Ohta model

Input Parameters	Remarks
Over Consolidation Ratio (OCR)	Over consolidation ratio
Pre-Consolidation Void Ratio (e_c)	Pre-consolidation void ratio
Slope of Consol. Line (λ)	Slope of normal consolidation line
Slope of Over Consol. Line (κ)	Slope of over-consolidation (swelling) line
Coefficient of dilatancy (D)	Coefficient of dilatancy
Coefficient of earth pressure at pre-consolidation (K_{0C})	Coefficient of earth pressure at rest at the time of pre-consolidation
Pre-Consolidation Vertical Stress(σ_{vc})	Pre-consolidation vertical stress

The over-consolidation ratio, OCR, above can be obtained from site investigation results, literatures, measured data and analysis of precedence of adjacent design. Under normal consolidation, OCR is set to 1.

The material properties, λ, κ listed in Table 3.9.1 are identical to the descriptions outlined for the Modified Cam-clay model in Figure 3.8.2.

As explained in the Modified Cam-clay chapter, the compression index and swelling index are determined by $\lambda = C_c / 2.303$ and $\kappa = C_r / 2.303$ of Eq. (3.8.1). In addition, λ and κ can be estimated from a graph of $\ln(p)$ versus void ratio instead of a graph of $\log_{10}(p)$ versus void ratio.

The coefficient of dilatancy, D can be calculated from triaxial CD tests under uniform pressure, p' using Eq. (3.9.1).

$$D = \frac{\lambda - \kappa}{M(1 - e_0)} \tag{3.9.1}$$

M is the slope of the critical state line, which can be calculated using the internal friction angle by Eq. (3.8.3).

The coefficient of earth pressure at rest at the time of pre-consolidation, K_{0C} can be obtained from triaxial K_0 consolidation tests.

3.9.2.2 Elasto-viscoplastic Material Properties

In addition to the elasto-plastic material properties, two additional properties are required to define the elasto-viscoplastic material model.

The coefficient of secondary consolidation, α can be determined by Oedometer tests.

Table 3.9.2 Elasto-viscoplastic material properties for Sekiguchi-Ohta model

Input parameters	Remarks
Coefficient of secondary consolidation (α)	
Initial volumetric strain ratio ($\dot{v}_0$)	

The initial volumetric strain ratio, $\dot{\nu}_0$ is the volumetric strain ratio at the time when secondary consolidation begins, which is given by,

$$\dot{\nu}_0 = \frac{\alpha}{t_0} \tag{3.10.2}$$

where, t_0 is the time when primary consolidation ends.

3.9.2.3 Auto-calculation of Material Properties

The Sekiguchi-Ohta model requires some material properties, which can be obtained only through difficult tests such as triaxial tests. SoilWorks automatically calculates such properties using other readily obtainable material properties.

Upon clicking “Auto-calculate Additional Parameters” as shown in Figure 3.9.1, the input dialog changes as shown in Figure 3.9.2.

SoilWorks provides the “Karibe” method and “Empirical” method in order to calculate the additional parameters.

Additional Parameters

☐ **Additional Parameters Auto-calculation**		
Calculation Method	Karibe	
Plasticity Index (PI)	30	
☐ Compression Index (Cc)	0.3	
☐ Recompression Index (Cr)	0.03	
☑ Preconsolidation Void Ratio	1	
Drain Distance (H)	1	m
Over-Consolidation Ratio (OCR)	1	
Slope of N.C. Line (λ)	0.3	
Slope of O.C. Line (K)	0.03	
Expansion Coefficient (D)	0.092	
Earth Pressure Coeff. (Koc)	1	
Secondary Consolidation Coeff.	0.005	
Initial Volumetric Strain Rate	1E-05	1/min
☐ Preconsolidation Vertical	0	kN/m²

Figure 3.9.1 Dialog for Additional Parameters

Additional Parameters

☑ **Additional Parameters Auto-calculation**		
Calculation Method	Karibe	
Plasticity Index (PI)	30	
☐ Compression Index (Cc)	0.3	
☐ Recompression Index (Cr)	0.03	
☑ Preconsolidation Void Ratio	1	
Drain Distance (H)	1	m
Over-Consolidation Ratio (OCR)	1	
Slope of N.C. Line (λ)	0.225	
Slope of O.C. Line (K)	0.03	
Expansion Coefficient (D)	0.064	
Earth Pressure Coeff. (Koc)	0.534	
Secondary Consolidation Coeff.	0.006	
Initial Volumetric Strain Rate	6.633E-08	1/min
☐ Preconsolidation Vertical	0	kN/m²

Figure 3.9.2 Auto-calculate Additional Parameters

Karibe Method

The Karibe equation basically requires the following input parameters:

Table 3.9.3 Input data for Karibe method

Input Parameters	Remarks	Applicable Models
Plastic index (I_p)		Elasto-plastic, Elasto-viscoplastic
Compression index (C_c)	Optional	Elasto-plastic, Elasto-viscoplastic
Slope of Over Consol. Line (κ)	Slope of over-consolidation (swelling) line	Elasto-plastic, Elasto-viscoplastic
Over consolidation ratio (OCR)		Elasto-plastic, Elasto-viscoplastic
Drainage distance (H)	Unit: cm	Elasto-viscoplastic

The following material properties are auto-calculated using the above parameters:

$$\lambda = 0.015 + 0.007 I_p \tag{3.9.3}$$

$$K_{0c} = 1 - \sin\phi' \tag{3.9.4}$$

$$D = \frac{\lambda\Lambda}{M\left(1+e_0\right)} \tag{3.9.5}$$

$$\alpha = \frac{\alpha_e}{1+e_0} \tag{3.9.6}$$

$$\dot{v}_0 = \frac{\alpha}{H^2 T_v\left(90\%\right)c_v} \tag{3.9.7}$$

Particular attention should be given that the unit of the drainage distance, H in Eq. (3.9.7) is fixed to cm. In case the compression index, C_c is user-defined, λ in Eq. (3.9.3) is calculated using the following equation:

$$\lambda = 0.434 C_c \tag{3.9.8}$$

M used in Eq. (3.9.3-7) is determined using Eq. (3.8.3). The internal friction angle, ϕ', the irreversibility ratio and the initial void ratio are calculated using the following equations:

$$\sin\phi' = 0.81 - 0.233\log I_p \tag{3.9.9}$$

$$\Lambda = M\ /1.75 \tag{3.9.10}$$

$$e_0 = 3.78\lambda + 0.156 \tag{3.9.11}$$

$$\alpha_e = 0.05/\lambda \tag{3.9.12}$$

$$\log c_v = -0.025 I_p - 0.25 \pm 1\left(cm^2/\min\right) \tag{3.9.13}$$

$$T_v\left(90\%\right) = 0.848 \tag{3.9.14}$$

Empirical Method

The empirical method requires the following parameters:

Table 3.9.4 Input data for Empirical method

Input Parameters	Remarks	Applicable Models
Plastic index (I_p)		Elasto-plastic, Elasto-viscoplastic
Compression index (C_c)		Elasto-plastic, Elasto-viscoplastic
Swelling index (C_r)	Optional	Elasto-plastic, Elasto-viscoplastic
Over consolidation ratio (OCR)		Elasto-plastic, Elasto-viscoplastic
Drainage distance (H)		Elasto-viscoplastic

The following properties are auto-calculated using the above parameters:

$$\lambda = 0.434 C_c \tag{3.9.15}$$

$$\kappa = \lambda / 10 \tag{3.9.16}$$

K_{0c} : Identical to Eq. (3.9.4)

D : Identical to Eq. (3.9.5)

α : Identical to Eq. (3.9.6)

$\dot{v}_0$: Identical to Eq. (3.9.7)

In case the swelling index, C_r is user-defined, Eq (3.9.16) is modified as below.

$$\kappa = 0.434 C_r \tag{3.9.17}$$

When using the auto-calculation function, the auto-calculated internal friction angle, ϕ' is used rather than using the user-defined angle.

3.9.3 Yield Function

3.9.3.1 Yield Function of Elasto-plastic Model

The yield function of the Sekiguchi-Ohta elasto-plastic model is as follows:

$$f\left(\boldsymbol{\sigma}', \varepsilon_v^p\right) = MD \ln \frac{p'}{p_0'} + D\eta^* - \varepsilon_v^p = 0 \tag{3.9.18}$$

where, ε_v^p is the plastic volumetric strain, and η^* is the generalized stress ratio, which is defined as,

$$\eta^* = \sqrt{\frac{3}{2}} \left\| \frac{\mathbf{s}}{p'} - \frac{\mathbf{s}_0}{p_0'} \right\| \tag{3.9.19}$$

where,

p'	: Average effective stress
$\mathbf{s}$	: Deviatoric stress vector
$\mathbf{s}_0$	: Deviatoric stress vector for pre-consolidation stress
p_0'	: Average effective stress for pre-consolidation stress

Figure 3.9.3 illustrates the yield surface shape of the Sekiguchi-Ohta model in the principal stress space.

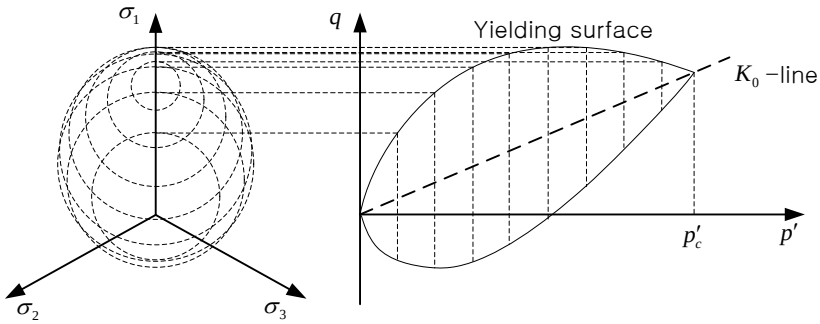

(a) Shape of yielding surface in deviatoric and meridian plane

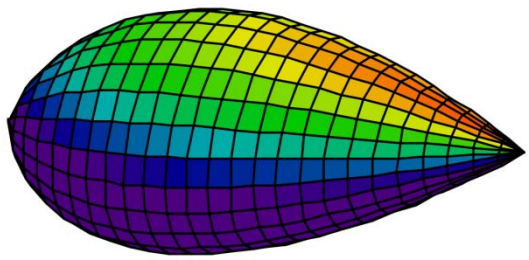

(b) 3D view in principal stress space

Figure 3.9.3 Yield surface shape of Sekiguchi-Ohta model

3.9.3.2 Yield Function of Elasto-viscoplastic Model

The yield function of the Sekiguchi-Ohta elasto- viscoplastic model is as follows:

$$f\left(\boldsymbol{\sigma}', \varepsilon_v^p\right) = \alpha \ln\left\{1 + \frac{\dot{v}_0 t}{\alpha} \exp\left(\frac{\overline{f}\left(\boldsymbol{\sigma}'\right)}{\alpha}\right)\right\} - \varepsilon_v^{vp} = 0 \tag{3.9.20}$$

where,

α	: Coefficient of secondary consolidation
$\dot{v}_0$	: Initial volumetric strain ratio
t	: Duration of consolidation

ε_v^{vp} : Viscoplastic volumetric strain

$\overline{f}(\boldsymbol{\sigma}')$ used in Eq. (3.9.20) is defined as follows using Eq. (3.9.18):

$$\overline{f}(\boldsymbol{\sigma}') = MD \ln \frac{p'}{p'_0} + D\eta^* \tag{3.9.21}$$

3.9.4 Initial Condition

The initial condition of the Cam-clay type of cohesive models is generally determined based on the pre-consolidation state. Therefore, determining the initial condition is thus a very important factor for these material models. In the case of the Sekiguchi-Ohta model, the soil modulus can separately consider the pre-consolidation state and the initial state. By reflecting p'_0 and $\mathbf{s}_0$ representing the initial stress in the yield function, the behavior of cohesive soil can be more accurately evaluated.

The effective stress at the initial state can be expressed as,

$$\boldsymbol{\sigma}'_i = \begin{Bmatrix} \sigma'_{iXX} \\ \sigma'_{iYY} \\ \sigma'_{iZZ} \\ \tau_{iXZ} \end{Bmatrix} \tag{3.9.22}$$

If the direction of gravity is defined as –Z axis, the vertical stress, σ'_{0ZZ} for pre-consolidation is calculated as follows:

$$\sigma'_{0ZZ} = \sigma'_{iZZ} \times OCR \tag{3.9.23}$$

Therefore, the effective stress, $\boldsymbol{\sigma}'_o$ for pre-consolidation can be formulated as follows:

$$\boldsymbol{\sigma}'_0 = \begin{Bmatrix} \sigma'_{0XX} \\ \sigma'_{0YY} \\ \sigma'_{0ZZ} \\ \sigma'_{0XZ} \end{Bmatrix} = \begin{Bmatrix} \sigma'_{Z0} \times K_{0C} \\ \sigma'_{Z0} \times K_{0C} \\ \sigma'_{Z0} \\ 0 \end{Bmatrix} \tag{3.9.24}$$

Using the above, p'_0 and $\mathbf{s}_0$ are given by,

$$p'_0 = \frac{\sigma'_{0XX} + \sigma'_{0YY} + \sigma'_{0ZZ}}{3}$$
$$\mathbf{s}_0 = \boldsymbol{\sigma}'_0 - p'_0 \mathbf{1} \tag{3.9.25}$$

where, $\mathbf{1} = \{1,1,1,0\}^T$

3.10 Modified Mohr-Coulomb Model

3.10.1 Introduction

The Modified Mohr-Coulomb model is an advanced material model that can simulate the behavior of different types of soil. It is based on an elasto-plastic formulation and can capture the basic properties of soil material, namely a pressure dependent shear strength (with soil dilatancy), irrecoverable compaction and nonlinear elastic unloading. This leads to a so-called double hardening model: One yield-surface for shear failure and one yield-surface for compaction. The Modified Mohr-Coulomb model combines power-law nonlinear elastic behavior, with exponential cap-hardening with Rowe's dilatancy rule and a parabolic hardening of the friction angle as function of the plastic shear-strain according to Duncan-Chang.

3.10.2 Material Properties

The parameters defining the Modified Mohr-Coulomb model are listed in Table 3.10.1.

Table 3.10.1 Input material property parameters for Modified Mohr-Coulomb model

Input parameters	Descriptions
Secant Stiffness in Tri-axial Test ($E50_{ref}$)	Reference secant stiffness in standard drained tri-axial test
Tangential Stiffness Primary Oedeometer Test ($Eoed_{ref}$)	Reference tangential stiffness for primary oedometer loading
Unloading/Reloading Stiffness (Eur_{ref})	Reference unloading/reloading stiffness
Reference Pressure (p_{ref})	Reference stress of the tri-axial test for the specified stiffness parameters
Ultimate Dilatancy Angle (ψ)	Ultimate dilatancy angle
Friction Angle at Shear (ϕ)	Internal friction angle at shear failure
Power of Stress Level Dependency (m)	Power of stress level dependency
Porosity (n)	Porosity
KNC ($KNC>0$)	K0 ratio for normally consolidated soil
Poisson's Ration (v)	Poisson ratio for unloading-reloading

3.10.3 Non-Linear Elasticity

The Modified Mohr-Coulomb model assumes power-law elastic volumetric stress-strain relation. That means that the elastic bulk modulus is defined as a power function of the hydrostatic pressure p :

$$K_t = K_{ref}\left(\frac{p+p_t}{p_{ref}}\right)^{1-m} \tag{3.10.2}$$

where

K_{ref} : Reference compression modulus

p_{ref} : Reference pressure from user input

m : power of stress level dependency from user input

p_t : Pressure shift for over-consolidation

Eq (3.10.2) leads to the following volumetric stress-strain relationship.

$$\left(\frac{p+p_t}{p_{ref}}\right)^{1-m} dp = K_{ref}\, d\varepsilon^e{}_v \tag{3.10.3}$$

Integration equation (3.10.3) results in

$$p = -p_t + ((p_0+p_t)^m - m p_{ref}{}^{m-1} K_{ref}\, \Delta\varepsilon_V{}^e)^{\frac{1}{m}} = F(\Delta\varepsilon_V{}^e) \tag{3.10.4}$$

The reference compression modulus is defined as:

$$K_{ref} = Eur_{ref}\,(\frac{3*KNC}{1+2*KNC})^m/(3-6*\nu) \tag{3.10.5}$$

and p_t is the pressure-shift which is defined as:

$$p_t = \frac{C}{\tan\phi} \tag{3.10.6}$$

3.10.4 Failure Criterion

The Modified Mohr-Coulomb model comprises 2 yield-surfaces which each have their own hardening function. A Mohr-Coulomb-like yield-surface f_1 with parabolic hardening function of the friction angle, starting from the user-defined initial internal friction angle ϕ_0 to the user-defined internal friction angle at shear failure ϕ, is defined for shear-failure. For compaction a cap-yield surface f_2 is defined with an exponential hardening function. Both yield-surfaces are defined in terms of p, q and the lode-angle θ.

$$\begin{aligned} f_1 &= \frac{q}{R_1(\theta)} - \frac{6\sin\phi}{3-\sin\phi}(p+\Delta p) = 0 \\ f_2 &= (p+\Delta p)^2 + \alpha\left(\frac{q}{R_2(\theta)}\right)^2 - {p_c}^2 = 0 \end{aligned} \tag{3.10.7}$$

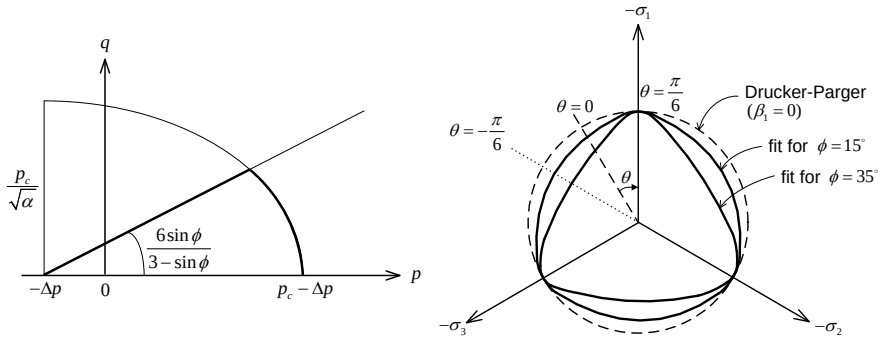

Figure 3.10.1 Projection of modified Mohr-Coulomb yield surface on two planes

in which the cap-shape factor

$$\alpha = \frac{2}{9}\frac{(1+2KNC)}{(1-KNC)}$$
$$\Delta p = \frac{C}{\tan\phi} \tag{3.10.8}$$

being the pressure shift. In midasGTS the parameter $R_1(\theta)$ is defined as follows:

$$R_1(\theta) = (\frac{1-\beta_1 \sin 3\theta}{1-\beta_1})^n \tag{3.10.6}$$

with n=-0.229 and the parameter β_1 defined as

$$\beta_1 = \frac{(\frac{3+\sin\phi}{3-\sin\phi})^{-\frac{1}{n}} - 1}{(\frac{3+\sin\phi}{3-\sin\phi})^{-\frac{1}{n}} + 1} \tag{3.10.7}$$

where the parameter β_1 is maximized to *0.7925*.

In midas GTS the parameter $R_2(\theta) = 1$.

3.10.5 Flow Rule

The direction of the plastic strain rate is determined by the plastic potential surfaces, where in case of the Modified Mohr-Coulomb model the following two surfaces are applied

$$q_1 = q - \frac{6\sin\psi}{3-\sin\psi}(p+\Delta p)$$
$$q_2 = (p+\Delta p)^2 + \alpha q^2 - p_c{}^2 \tag{3.10.9}$$

which implies an associative behavior in the *p*-*q* space and a non-associated flow in the deviatoric space. The dilatancy angle ψ is related to the friction angle ϕ by the assumption of Rowe's stress dilatancy theory, which reads

$$\sin\psi = \frac{\sin\phi - \sin\phi_{cv}}{1 - \sin\phi \sin\phi_{cv}} \tag{3.10.10}$$

in which $\sin\phi_{cv}$ a constant value which can be conceived as the friction angle at constant volume.

Chapter 4

Seepage Constitutive Models

4.1 Permeability Coefficient Function

Ground water in a fluid state is entangled as a net, which flows through continuous inter-connected flow channels. As the water content decreases, the effect of a decrease in the size and number of water channels appears, resulting in a decrease in the total amount of water flow within the soil. In an extreme condition of dry soil, the permeability of water through the flow channels disappears, whereas the permeability reaches the maximum in saturated soil since all the flow channels become effective.

The amount of seepage flow can be determined by the permeability coefficient using the Darcy's law. However, the permeability coefficient for seepage flow in unsaturated soil depends on the water content. The permeability coefficient reaches the maximum when the soil becomes saturated and tends to rapidly decrease with the decrease in water content. The water content is a function of pore water pressure, and the permeability coefficient is a function of water content. Hence the permeability coefficient becomes a function of pore water pressure. Figure 4.1.1 shows a classical relationship between the permeability coefficient and pore water pressure.

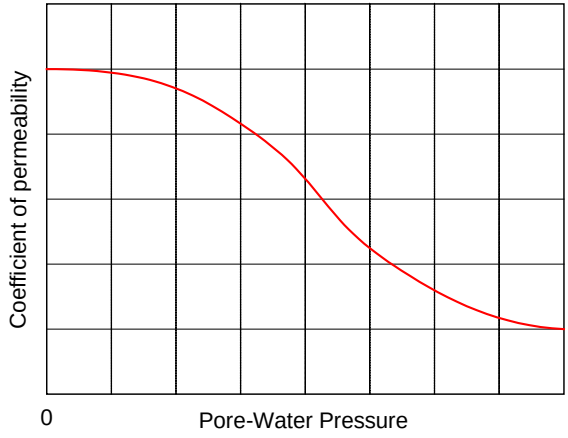

Figure 4.1.1 Permeability coefficient function

4.2 Volumetric Water Content Function

When water flows through the soil, a certain amount of water is retained in the ground structure. The amount of the water is governed by the capillary absorption force of the soil and the property of the ground structure. In seepage analysis, this water content is better expressed as the volumetric water content, which is a ratio of the volume of water to the total volume.

$$\Theta = V_w / V \tag{4.2.1}$$

where,

Θ : Volumetric water content

V_w : Volume of water

V : Total Volume

The relationship curve between the volumetric water content and the pore water pressure is known as the water content characteristic curve as shown in Figure 4.2.1. The slope of the curve, m_w , represents the rate of change in the amount of water retained in the soil with the change in pore water pressure.

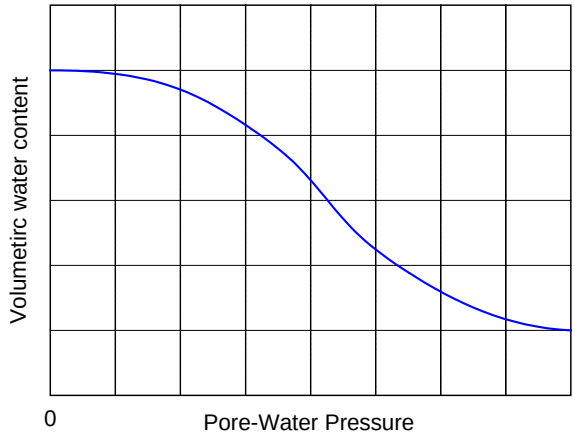

Figure 4.2.1 Water content characteristic curve

$$\Theta_w = \Theta_r + \frac{\left(\Theta_s - \Theta_r\right)}{\left[1+\left(\alpha h\right)^n\right]^m} \tag{4.2.2}$$

Where,

Θ_w : Unsaturated volumetric water content

Θ_s : Saturated volumetric water content

Θ_r : Residual volumetric water content

α , n , m : Curve shape factors (α =1/unit length, $m = 1 - 1/n$)

h : Negative (-) pore water pressure head

When the soil is 100% fully saturated, the volumetric water content becomes the same as the porosity, and it can be represented as the ratio of the volume of pores to the total volume.

In the case of fully saturated soil with the pore water pressure close to zero under constant external force, if the pore water pressure increases and becomes positive, the effective stress decreases, and the volume of soil increases. As a result, the water content in the soil increases. On the other hand, if the pore water pressure decreases to a negative value, the water content decreases due to the drainage of water. Ultimately, even if the pore water pressure further decreases after the water is completely drained from the soil, no further change in water content takes place.

The slope (m_w) of the water content characteristic curve represents the variation of water content in soil with the change in pore water pressure head.

4.3 Consecutive Function

Both the 4.1 permeability coefficient function and 4.2 volumetric water content function were defined using the pressure head function alone. However in reality, both the volumetric water content and the permeability coefficient are influenced by the change in water pressure head in the soil of nonlinear behavior. Therefore, SoilWorks provides a consecutive function that considers the permeability coefficient based on the water content by defining a function of “pressure head-water content-permeability coefficient” and obtaining the change in water content relative to the pressure head. Likewise, SoilWorks provides the function of “pressure head-degree of saturation-permeability coefficient” using the relation of the water content and the degree of saturation.

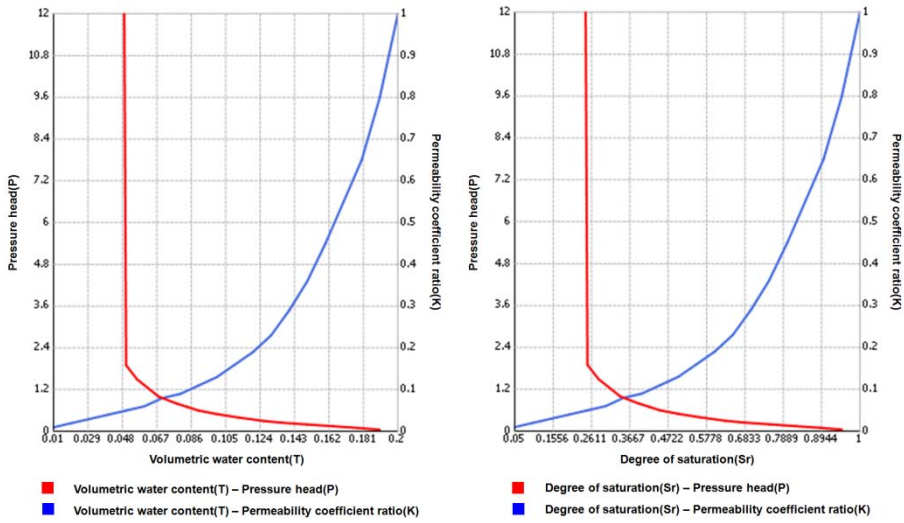

(a) Pressure head-water content -permeability coefficient ratio

(b) Pressure head-degree of saturation -permeability coefficient ratio

Figure 4.3.1 Consecutive function

Appendix

A. Output of Safety Ratio

As a convenient post-processing feature, SoilWorks produces the safety factor that enables the user to check the safety of a model. This function does not affect other analysis results. This function can be used only with Tunnel Module and is available for all the material models.

The safety factor is defined as the ratio of the current stress state to the stress at failure. The Mohr-Coulomb failure criterion is used, which is most commonly used for brittle materials such as soils. As shown in Figure A.1, failure is assumed to occur when a Mohr circle A, which represents the stress at a point in soil, meets the straight line B defined by the Coulomb's friction law.

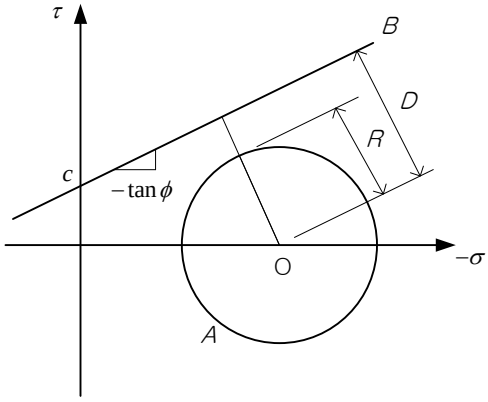

Figure A.1 Mohr-Coulomb failure criterion

The expression of safety factor based on the Mohr-Coulomb's failure criterion is as follows:

$$f = \frac{D}{R} \tag{A.1}$$

where,

R : Radius of Mohr circle

D : Distance from the center of Mohr circle to Line B

If the state of stresses is $\left\{\sigma_{xx}, \sigma_{yy}, \sigma_{zz}, \tau_{xz}\right\}^T$ with the model being on the X-Z plane, $\sigma_{zz} > \sigma_{xx}$ and the direction of gravity in –Z axis, the Mohr circle is drawn as follows:

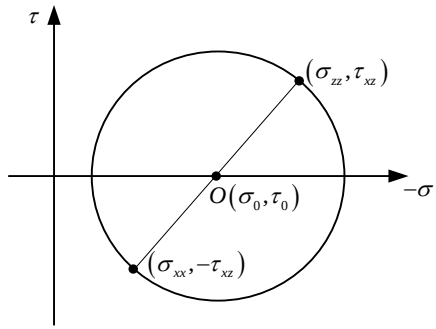

Figure A.2.Mohr circle representing stresses

Using Figure A.2, the radius, R and the center distance, D of the Mohr circle illustrated in Figure A.1 can be calculated as follows:

$$\sigma_0 = \frac{(\sigma_1 + \sigma_2)}{2} \tag{A.2}$$

$$R = \sqrt{(\sigma_1 - \sigma_0)^2 + \tau^2} \tag{A.3}$$

$$D = \frac{|\tau_0 - c + \sigma_0 \tan\phi|}{\sqrt{c^2 + (\tan\phi)^2}} \tag{A.4}$$

where,

σ_0 : Stress at the center of Mohr circle

σ_1 : Maximum principal stress

σ_2 : Minimum principal stress

c : Cohesion used for safety factor calculation

ϕ : Friction angle used for safety factor calculation

As an exception to the above, if the maximum/minimum principal stresses are at the hydrostatic line, the Mohr circle becomes a point, and consequently the safety factor cannot be computed in which case the safety factor of -1 is assigned. If the center of the Mohr circle is located beyond the tension zone, the safety factor of -2 is assigned.

B. Output of Plastic State

This function displays the plastic state more intuitively. Since the failure criteria are different from material to material, elastic state and plastic state are separately displayed as shown in the table below. In addition, as the status of the progress of stress depends on the state of loading or unloading, the stress at the integration point is displayed with the distinction of loading, unloading or tension failure.

Duncan-Chang

State	State Variable	Post Symbol
Elastic	11	
Failure	12	△
Unloading or reloading	13	⊿
Tension	14	⊹

Mohr-Coulomb

State	State Variable	Post Symbol
Elastic	31	
Plastic	32	○
Unloading or reloading	33	⦶
Tension failure	34	⊕

Drucker-Prager

State	State Variable	Post Symbol
Elastic	41	
Plastic	42	
Unloading or reloading	43	
Tension failure	44	

Modified Cam-Clay

State	State Variable	Post Symbol
Elastic	61	
Plastic	62	
Unloading or reloading	63	

Hoek-Brown

State	State Variable	Post Symbol
Elastic	71	
Plastic	72	
Unloading or reloading	73	

Von Mises

State	State Variable	Post Symbol
Elastic	81	
Plastic	82	
Unloading or reloading	83	

Tresca

State	State Variable	Post Symbol
Elastic	91	
Plastic	92	⬠
Unloading or reloading	93	⬠

Sekiguchi-Ohta

State	State Variable	Post Symbol
Elastic	101	
Plastic	102	◇
Unloading or reloading	103	◫
Tension failure	104	⊕